

Carbon Pricing and Monetary Policy in an Estimated Macro-Climate Model*

[Link to most recent version](#)

Sofia Semik[†]

November 12, 2025

Abstract

I develop and estimate a heterogeneous-agent New Keynesian macro-climate model to study the effects of carbon price shocks on the euro area. Using EU ETS data and local projections, I document three empirical results of carbon price shocks: a gradual decline in emissions, a temporary surge in inflation, and a contraction in economic activity. Four key mechanisms allow the model to reproduce these results: fossil energy adjustment costs, limited substitutability between fossil and green energy, complementarities between energy and other inputs, and the presence of Hand-to-Mouth households vulnerable to higher energy prices. These model features crucially shape the optimal monetary policy response. Carbon price shocks pose a monetary policy trade-off: raising interest rates would curb inflation but deepen the demand contraction. The Ramsey planner instead cuts the policy rate, accepting temporarily higher inflation to stabilize real activity. Absent the key model features, a rate hike becomes optimal. A Taylor rule targeting core rather than headline inflation is closer to the welfare-optimal response.

JEL Codes: E52, H23, Q43, Q58

Keywords: Carbon pricing, optimal monetary policy, Bayesian estimation

*I'm grateful for the comments and suggestions from colleagues, and from participants of the ECB Conference on Monetary Policy 2025, the 2nd International Conference on the Climate-Macro-Finance Interface and the EEA 2025 Annual Congress, and especially for the continuous feedback and support I received from my supervisor Mathias Trabandt. I am very grateful for the hospitality and guidance of Diego Käning at Northwestern University, where parts of this paper were written during a research visit in the fall of 2024.

[†]Goethe University Frankfurt, Email: sofia.semik@gmail.com, Website: sofiasevik.com

1 Introduction

To address the growing urgency of climate change, governments increasingly rely on carbon pricing to foster the transition to a low-carbon economy with sustainable energy production. Despite growing research on the macroeconomic effects of carbon price increases, important questions remain, especially regarding its role in driving “greenflation”, the inflationary pressures from climate mitigation policies (Schnabel, 2022). These inflationary pressures pose a challenge for monetary policy, as central banks must respond to the macroeconomic effects of climate change mitigation policies while remaining consistent with their price stability mandates. Developing models that accurately capture the empirical transmission of carbon pricing is therefore essential for effective monetary policy design.

In this paper, I develop and estimate a heterogeneous-agent New Keynesian macro-climate model with energy that accounts for macroeconomic effects of carbon price increases in the euro area observed in the data. I assess the macroeconomic impact of carbon price increases on the EU Emission Trading System (EU ETS) carbon market using local projections. For this I use the carbon price shock time series constructed by Käenzig (2023), which identifies unexpected changes in ETS emission allowance future prices. My findings suggest that carbon price shocks effectively reduce greenhouse-gas (GHG) emissions, though the reduction is not immediate. Instead, emissions decline gradually, likely due to technological constraints and infrastructure limitations that prevent an instantaneous shift away from fossil energy. However, the emission reduction comes at an economic cost for the euro area. The carbon price shock triggers a sharp increase in energy prices, leading to an immediate rise in headline inflation. Higher energy costs raise production expenses for firms and increase households’ energy bills, causing a decline in economic activity. The fall in wages, stemming from firms’ higher energy-related costs, further reduces household income, amplifying the drop in consumption and aggregate demand.

To accurately capture these empirical results, I develop a heterogeneous-agent New Keynesian model with a disaggregated energy sector. The economy features Ricardian and Hand-to-Mouth households, firms producing intermediate and final goods, and energy producers supplying fossil and green energy. Fossil energy use generates carbon emissions, while green energy production is carbon-neutral, and emissions reduce total factor productivity through environmental damage. A composite of green and fossil energy enters both production and household consumption. Carbon policy is modeled as a surcharge on fossil energy prices. I estimate my model using Bayesian impulse response matching. This methodology involves minimizing the distance between the dynamic responses of the model to a carbon price shock and analog objects in the data obtained from the local projections. The model accounts well for the key empirical features of

the estimated impulse response functions: a gradual decline in emissions, an immediate surge in headline inflation and a significant drop in economic activity. The following model features are key to accounting for the empirical results:

The model incorporates quadratic adjustment costs for fossil energy use, preventing an immediate contraction in fossil energy demand after a carbon price shock. The estimated adjustment cost parameter is significantly positive, and these frictions are essential to replicate the gradual decline in emissions observed in the data. A possible interpretation is that these costs capture technological and infrastructure constraints that slow the transition away from fossil energy. Second, the estimated elasticity of substitution between green and fossil energy is below unity in my model, indicating that these energy sources are complements rather than substitutes. The low short-term substitutability in response to temporary shocks in my model is essential to capturing the strong pass-through from fossil energy prices to aggregate energy prices. Higher substitutability would imply a weaker inflationary response, leading to a counterfactually small rise in headline inflation and associated decline in aggregate demand. Third, there is very strong complementarity of energy in production and consumption. The model assumes that energy is a crucial input for both firms and households, making it difficult to substitute away from energy consumption. This amplifies the economic effects of carbon price shocks, as it makes households and firms more vulnerable to higher energy prices following carbon price shocks. Finally, including Hand-to-Mouth households into the model helps explaining the significant drop in consumption observed in the data, because they are more vulnerable to energy price increases.

These features are crucial not only for matching the empirical responses but also for shaping optimal monetary policy in response to carbon price shocks. I compare the implications of a welfare-maximizing Ramsey monetary policy with alternative interest rate rules in response to a carbon price shock. The results highlight a key trade-off for monetary policy: stabilizing inflation would require higher interest rates, but this would amplify the contraction in aggregate demand. The Ramsey planner instead places greater weight on stabilizing real activity by cutting interest rates and accepting temporarily higher inflation to cushion the decline in demand. In contrast, a model without the key features described above implies a much smaller policy rate cut in response to the shock, and can even call for a rate hike. The key intuition is that without these features, the model cannot capture the pronounced effect of carbon price shocks on aggregate demand. Greater substitutability between fossil and green energy, or between energy and other inputs and goods, as well as the absence of Hand-to-Mouth households, substantially weaken the demand effects of the shock, implying a much smaller optimal rate cut. Removing fossil energy adjustment costs further amplifies the initial inflation surge. When all of these features are absent, the optimal monetary policy response switches to a rate hike.

A Taylor rule that stabilizes core instead of headline inflation comes closer to the optimal monetary policy response. By focusing on core inflation, the central bank effectively “looks through” the temporary surge in energy inflation, avoiding excessive monetary tightening and thus mitigating the fall in demand. While this approach leads to a somewhat larger initial increase in headline inflation, this effect is small and not persistent.

This paper contributes to the growing macro-climate DSGE literature by providing an empirically grounded framework for evaluating the macroeconomic effects of carbon pricing in the euro area. The findings are particularly relevant for the design of monetary policy in the face of inflationary pressures and output losses arising from climate policy initiatives.

Related Literature. This paper contributes to both empirical and theoretical literature on the macroeconomic effects of climate change mitigation policies and potential implications for monetary policy. First, my paper is related to a growing strand of empirical literature assessing the macroeconomic effects of carbon price increases. The empirical part is closely related to Käenzig (2023). Käenzig uses high-frequency identification of regulatory events on the European carbon market to construct a carbon policy surprise shock series and studies the effects on the euro area economy and on emissions. His findings suggest that an increase in the EU ETS carbon price is effective in reducing emissions, but entails economic costs as it creates inflationary pressures and a fall in employment and real activity. Metcalf and Stock (2023) analyze the macroeconomic implications of European carbon taxes. Interestingly, they find that while carbon taxes reduce emissions, they do not lead to a significant reduction in GDP. Similarly, Konradt and Weder di Mauro (2023) do not find evidence for significant inflationary pressures caused by carbon taxes using data from European and Canadian carbon tax regimes. Gagliardone and Gertler (2023) estimate a New Keynesian model to match the empirical impulse responses to an oil shock. Their findings suggest that strong complementarity of oil in production and consumption are key to account for the macroeconomic dynamics following an oil price increase. I contribute to this literature by assessing the impact of EU ETS carbon price increases on emissions and the macroeconomy and using these results to estimate a New Keynesian macro-climate model with a disaggregated energy sector.

The second related strand of literature focuses on developing New Keynesian models with an explicit energy sector to assess the impact of carbon price increases on inflation and the conduct of monetary policy. Sahuc et al. (2025) estimate a stylized New Keynesian climate model without an explicit energy sector to analyze long-term transition scenarios and their implications for inflation and monetary policy under different climate policy regimes. Coenen et al. (2024) extend the ECB’s New Area-Wide Model with a disaggregated energy sector to assess the impact of different carbon transition paths on

the euro area economy. Their results suggest an increase in headline inflation and a fall in aggregate demand during the transition due to the increase in energy prices. Similarly, Olovsson and Vestin (2023) find that it is optimal for euro area monetary policy to see through increasing energy prices and focus on stabilizing core inflation, which leads to an increase in headline inflation. However, their results suggest that this increase is modest as long as the carbon tax path is pre-announced. Del Negro et al. (2023) develop a two-sector model to study how the green transition affects the central bank’s trade-off between keeping prices stable and closing the output gap. Nakov and Thomas (2023) study Ramsey optimal monetary policy in a model with climate externalities and how it is affected by different environmental policy regimes. Diluiso et al. (2021) analyze the macroeconomic impact of the green transition under different monetary policy rules using an estimated model for the euro area. I contribute to this literature by estimating a model that is capable of accounting for the effects of carbon price shocks observed in the data and analyzing the optimal monetary policy response to these shocks.

Structure. The remainder of the paper is structured as follows: Section 2 presents empirical evidence on the macroeconomic effects of a carbon price shock in the euro area. Section 3 develops the New Keynesian macro-climate model with energy. Section 4 outlines the estimation methodology, presents the model estimation results and discusses the importance of key parameters. Section 5 analyzes the optimal monetary policy response to carbon price shocks and evaluates the impact of alternative monetary policy rules. Section 6 concludes.

2 Empirical Analysis

In this section, I assess the macroeconomic implications of an increase in the EU ETS carbon price in the euro area. The EU ETS operates as a carbon market where a fixed number of emission allowances are issued, granting firms the right to emit greenhouse gases into the atmosphere. Firms can buy, sell, and trade these allowances, creating a market-driven price for carbon emissions. To identify changes in the ETS price, I rely on the carbon price shock time series developed by Käenzig (2023), which captures unexpected variations in emission allowance futures prices using high-frequency surprise changes. It is a monthly shock series that spans from 1999 to 2019. I aggregate the monthly carbon price shock time series to quarterly frequency to match the frequency of macro data such as GDP and private consumption. I estimate the effects using local projections (Jordà, 2005):

$$y_{i,t+h} = \beta_{h,0}^i + \gamma_h^i CPShock_t + \sum_{\ell=1}^p \beta_{h,\ell}^i y_{i,t-\ell} + \delta_h^i t + \epsilon_{i,t,h}, \quad (1)$$

where $CPShock_t$ denotes the ETS carbon price shock time series. The coefficient γ_h^i measures the response of variable i at horizon h to a carbon price shock. I include three lags of the dependent variable as controls ($p = 3$). The term $\delta_h^i t$ accounts for time trends over the sample. The estimation is based on quarterly euro area data from 1999Q1 to 2019Q4, focusing on the impact of carbon price increases on inflation, greenhouse gas emissions, and real activity.

The variables included in the local projections are HICP energy inflation, headline HICP inflation, HICP inflation excluding energy, the real fossil energy price, greenhouse gas emissions, industrial energy production, the policy rate, real GDP, real private consumption, real investment, real wages, and capacity utilization. Inflation and the interest rate are expressed in annualized rates, while all other variables are measured in log-levels, except for capacity utilization. The real fossil energy price is constructed as a weighted index of the Brent crude oil price and the HICP gas component, deflated by headline HICP. For the policy rate, I splice the ECB policy rate with the shadow rate from Wu and Xia (2020) to account for the period when the policy rate was constrained by the zero lower bound. Since GHG emissions are only available annually, I construct a quarterly series using the Chow–Lin temporal disaggregation method with indicators, applying the code from Quilis (2024). Following Käenzig (2023), I use the HICP energy component and industrial production as quarterly indicators. Industrial energy production is measured as the real volume of output in the energy sector. All data sources are outlined in Appendix A. The shock used in the local projections is normalized to raise annualized energy inflation by one percentage point on impact¹. The confidence bands are computed using the lag-augmentation method of Montiel Olea and Plagborg-Møller (2021).

Figure 1 shows the impulse responses to a carbon price shock for inflation, GHG emissions, and industrial energy production. The shock triggers an immediate rise in fossil energy prices and, consequently, aggregate energy prices. The pass-through of energy prices to consumer prices appears to be strong, as headline inflation increases by about 0.15 percentage points on impact. Inflation excluding energy also rises slightly, reflecting higher production costs being passed on to consumers. The carbon price increase proves effective in curbing emissions, with GHG emissions falling significantly by as much as 0.25 percent. Interestingly, this adjustment does not occur immediately but unfolds gradually, with the trough reduction materializing only one year after the shock. A very similar pattern is observed for industrial energy production, which contracts in response to the shock along almost the same trajectory. This co-movement is intuitive, as a large share of emissions originates from the combustion of fossil fuels in energy production. When higher carbon prices make fossil-based energy production more costly, industrial energy

¹Figure B.1 in the Appendix shows that this corresponds to approximately 0.3 standard deviations of the identified carbon price shock, indicating that the normalized shock represents a relatively small disturbance. Even a shock an order of magnitude larger would remain within the empirically plausible range.

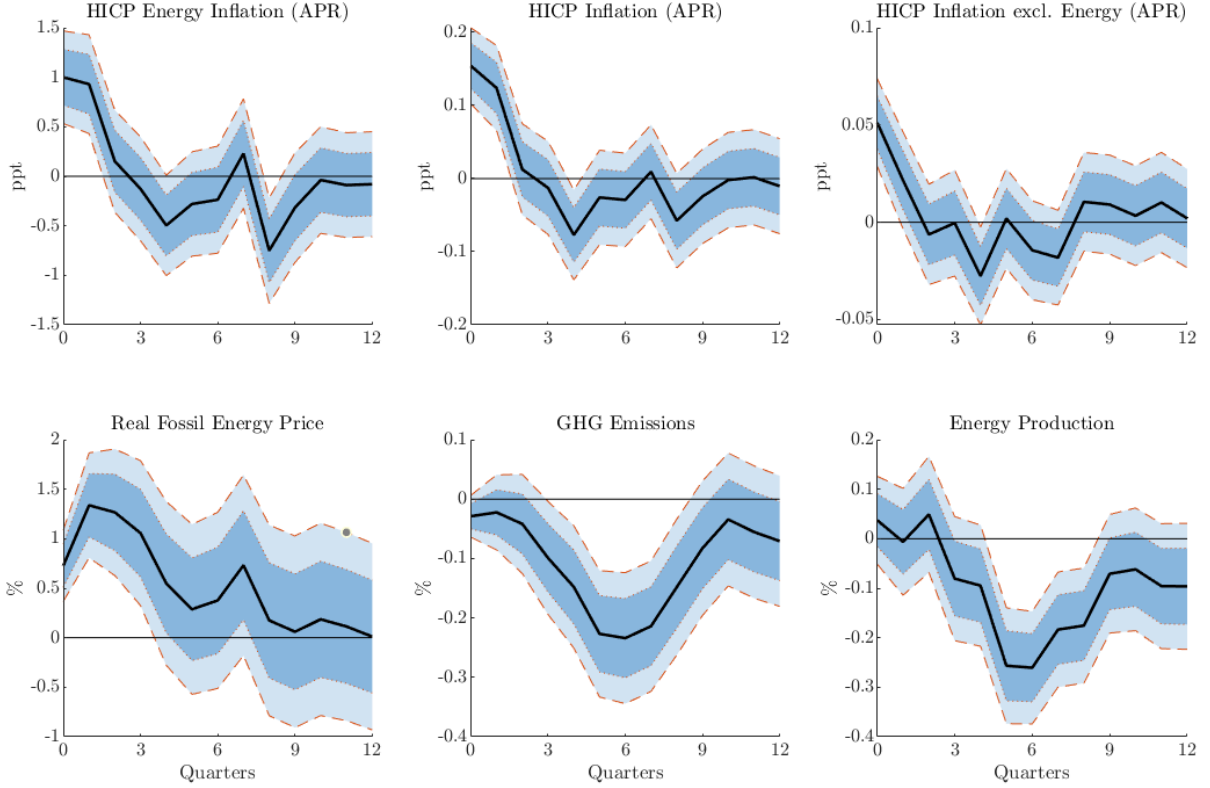


Figure 1: Impulse responses of prices, emissions and energy

Notes: The solid line is the point estimate, the dark and light shaded areas are 68% and 90% confidence bands. The shock is normalized to increase annualized energy inflation by 1 ppt on impact.

output declines, and emissions fall accordingly. The delayed adjustment suggests that the reduction in fossil energy use unfolds gradually, leading both series to trough with a lag. In terms of both direction and magnitude, these results are consistent with Käenzig (2023) as well as previous evidence on different energy price shocks, such as oil shocks (Käenzig (2021), Baumeister and Hamilton (2019)).

The results indicate a strong pass-through from fossil energy to consumer prices. Figure 2 presents the responses of several macroeconomic aggregates to the same carbon price shock. Real GDP declines significantly, with a peak reduction of about 0.15 percent, driven by contractions in both consumption and investment. Real wages and capacity utilization in production also fall. Higher energy prices directly reduce the disposable income of households and raise firms' marginal costs, leading to lower consumption and investment. The resulting fall in demand prompts firms to scale back production, which puts downward pressure on wages. The delayed but pronounced decline in real wages shown in Figure 2 illustrates this adjustment, and the associated drop in labor income further weakens aggregate demand. According to Käenzig (2023), these indirect general equilibrium effects that operate through wages and income rather than direct energy costs explain more than two-thirds of the fall in consumption. This mechanism helps account for the strong real effects of carbon price shocks. Contractionary monetary policy in

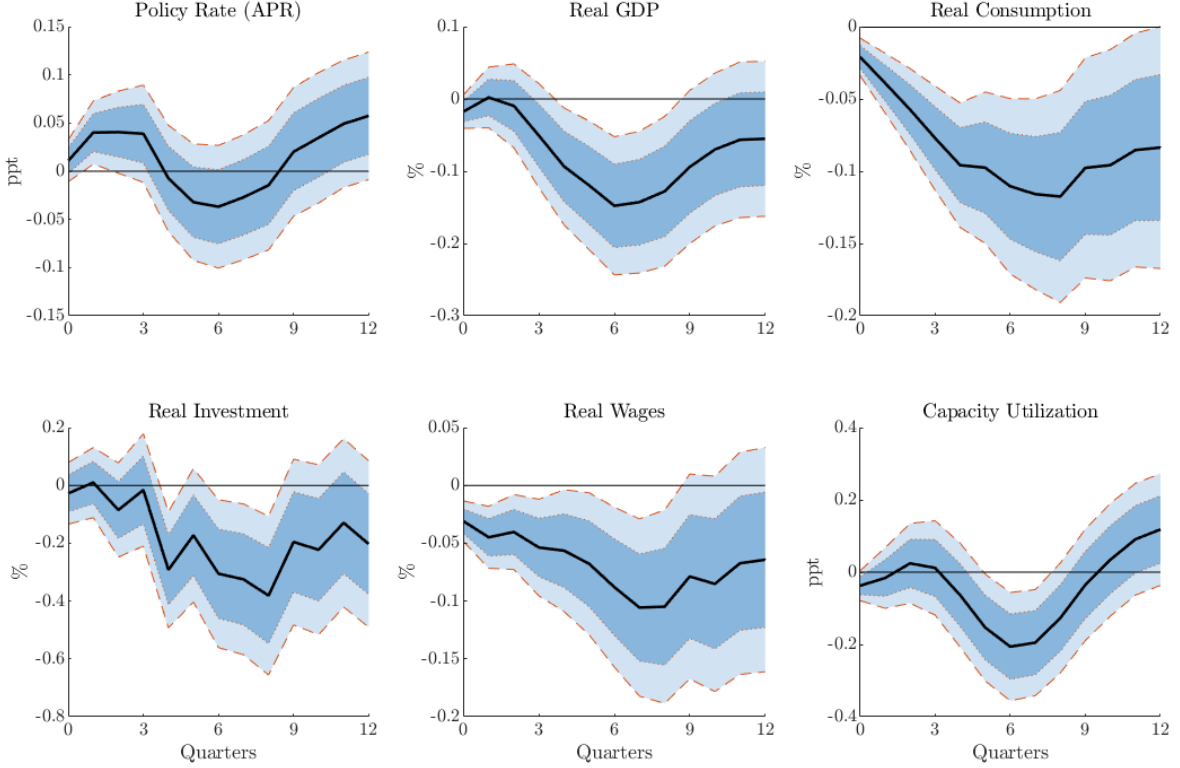


Figure 2: Impulse responses of macroeconomic aggregates

Notes: The solid line is the point estimate, the dark and light shaded areas are 68% and 90% confidence bands. The shock is normalized to increase annualized energy inflation by 1 ppt on impact.

response to inflationary pressures from higher energy prices represents another potential transmission channel, although the estimated policy rate response is small and mostly insignificant.

The main results are robust to alternative specifications shown in Appendix B.2. Figure B.2 presents estimates using four rather than three lags as controls ($p = 4$), which yield results very close to the baseline. Figure B.3 reports impulse responses based on log-differences rather than log-levels to address potential concerns about non-stationarity. The local projections are estimated in log-differences and then cumulated to make the responses comparable to the baseline specification. The results in Figure B.3 show that the point estimates are nearly identical to those in the baseline, while the confidence intervals are somewhat narrower for most variables.

3 The Model

The macro-climate model is a heterogeneous-agent New Keynesian framework with nominal price and wage rigidities, extended by an energy sector. The economy is populated by Ricardian and Hand-to-Mouth households, final good producers, intermediate good producers, and producers of green and fossil energy. Fossil energy production generates carbon emissions, while green energy is carbon-neutral. Carbon emissions reduce

total factor productivity through environmental damage. A composite of green and fossil energy enters both intermediate goods production and household consumption. Carbon policy is implemented as a surcharge on the price of fossil energy.

3.1 Households

The model features two types of households: a constant share λ of Hand-to-Mouth households (H) and a share $1 - \lambda$ of Ricardian households (R). Ricardian households optimize intertemporally, have access to financial markets and supply capital and labor. Their preferences are specified as:

$$\mathbb{E}_0 \sum_{t=0}^{\infty} \beta^t \left\{ \ln(c_{t,R} - bc_{t-1,R}) - \frac{h_{t,R}^{1+\varphi}}{1+\varphi} \right\}, \quad (2)$$

where $c_{t,R}$ represents final consumption, $h_{t,R}$ represents hours worked, $\beta \in (0, 1)$ is the discount factor, b controls the degree of habit formation and φ is the inverse Frisch elasticity.

The R household's budget constraint is defined as follows:

$$\sum_j P_{t,R} c_{t,R} + P_t^I i_t^j + B_{t+1} = W_t h_{t,R} + (R_t^{k,j} u_t^j - a(u_t^j) P_t^I) k_{t-1}^j + R_{t-1} B_t + T_{t,R} + \Pi_t, \\ j \in (Y, G, B) \quad (3)$$

Here, $P_{t,R}$ is the nominal price of final consumption goods and P_t^I is the nominal price of investment goods i_t^j . Investment is allocated across three different sectors: capital goods for intermediate goods production k_t^Y , green energy production k_t^G and fossil energy production k_t^B . R_t^k is the nominal rental rate of capital and $u_t^j K_t^j$ denotes the household's supply of capital services in the given period, where u_t^j is the capacity utilization rate. $a(u_t^j)$ denotes cost of capacity utilization in units of investment goods. R households can invest in one-period risk-free bonds B_{t+1} , where $R_{t-1} B_t$ denotes the revenue from holding bonds. $W_t h_{t,R}$ is household R ' labor income, $T_{t,R}$ are lump-sum transfers directed towards R agents and Π_t are firm profits.

Following Christiano et al. (2005), R households face quadratic adjustment costs in investment, so that investment is smoothed over time. This results in the following law of motion for capital in each sector:

$$k_t^j = (1-\delta) k_{t-1}^j + \left[1 - \frac{\kappa_I}{2} \left(\frac{i_t^j}{i_{t-1}^j} - 1 \right)^2 \right] i_t^j, \quad j \in (Y, G, B) \quad (4)$$

where κ_I denotes the investment adjustment cost parameter, which I assume is identical across sectors.

Labor supplied by individual households is differentiated, which yields the following expression for aggregate labor supply:

$$h_{t,R} = \left(\int_0^1 h_{t,R}(i)^{\frac{\varepsilon_W - 1}{\varepsilon_W}} di \right)^{\frac{\varepsilon_W}{\varepsilon_W - 1}}, \quad (5)$$

where ε_W is the elasticity of substitution between individual labor varieties.

Ricardian households are assumed to set wages in a Calvo-style staggered fashion. Each period household i is able to reoptimize its nominal wage rate with probability $1 - \theta_W$. The remaining fraction of households cannot reoptimize, such that $W_t(i) = W_{t-1}(i)\pi$ with probability θ_W . The optimal wage-setting problem is derived in Appendix C.1.

The second type of households are Hand-to-Mouth, meaning they do not optimize intertemporally and have no access to financial markets. Instead, they consume their entire disposable income each period. Their preferences are specified analogously to those of Ricardian households:

$$\mathbb{E}_0 \sum_{t=0}^{\infty} \beta^t \left\{ \ln(c_{t,H} - bc_{t-1,H}) - \frac{h_{t,H}^{1+\varphi}}{1+\varphi} \right\}, \quad (6)$$

where $c_{t,H}$ denotes Hand-to-Mouth consumption and $h_{t,H}$ denotes hours worked by H households. All preference parameters are assumed to be identical to those of R households.

The H household's budget constraint reads as follows:

$$P_{t,H} c_{t,H} = W_t h_{t,H} + T_{t,H},$$

where $T_{t,H}$ are transfer payments directed towards H households. Following Erceg et al. (2024), I assume that H agents have no bargaining power and do not optimize their hours worked, but instead work the same hours as R agents, $h_{t,H} = h_{t,R}$ to earn the economy-wide wage W_t . Including Hand-to-Mouth agents in the model is crucial to account for potentially large demand-side effects of energy price shocks (see Auclert et al. (2023), Chan et al. (2024), Käenzig (2023)).

To capture energy consumption of households, final consumption $c_{t,i}$ is a CES bundle of energy ($c_{t,i}^E$) and manufactured goods from final good production ($c_{t,i}^X$):

$$c_{t,i} = \left(\gamma_{c,i}^{\frac{1}{\varrho_c}} (c_{t,i}^E)^{\frac{\varrho_c-1}{\varrho_c}} + (1 - \gamma_{c,i})^{\frac{1}{\varrho_c}} (c_{t,i}^X)^{\frac{\varrho_c-1}{\varrho_c}} \right)^{\frac{\varrho_c}{\varrho_c-1}}, \quad i \in \{H, R\}. \quad (7)$$

Here, $\gamma_{c,i}$ determines the steady-state share of energy in final consumption, which is heterogeneous across household types, and ϱ_c is the elasticity of substitution between energy and the manufactured good. The resulting demand equations for energy and the manufactured consumption good are given by:

$$c_{t,i}^E = \gamma_{c,i} \left(\frac{P_t^E}{P_{t,i}} \right)^{-\varrho_c} c_{t,i}, \quad (8)$$

$$c_{t,i}^X = (1 - \gamma_{c,i}) \left(\frac{P_t^X}{P_{t,i}} \right)^{-\varrho_c} c_{t,i}, \quad (9)$$

where P_t^E and P_t^X is the price of energy and the price of non-energy goods, respectively. The aggregate consumer price for each household is defined as:

$$P_{t,i} = (\gamma_{c,i}(P_t^E)^{1-\varrho_{c,j}} + (1 - \gamma_{c,i})(P_t^X)^{1-\varrho_c})^{\frac{1}{1-\varrho_c}}. \quad (10)$$

The economy-wide CPI is given by:

$$P_t = \lambda P_{t,H} + (1 - \lambda) P_{t,R}, \quad (11)$$

where $\lambda \in [0, 1]$ denotes the share of Hand-to-Mouth agents.

3.2 Final good firms

The representative final-good firm uses the following CES bundle to produce the final good y_t :

$$y_t = \left(\int_0^1 y_t(z)^{\frac{\varepsilon-1}{\varepsilon}} dz \right)^{\frac{\varepsilon}{\varepsilon-1}}, \quad (12)$$

where $y_t(z)$ is an intermediate good produced by intermediate good firm z and ε is the elasticity of substitution between intermediate goods. The profit maximization problem of the final good firm reads as follows:

$$\max_{y_t, \{y_t(z)\}_{z \in [0,1]}} P_t^X y_t - \int_0^1 P_t^X(z) y_t(z) dz \quad (13)$$

$$\text{s.t. } y_t = \left(\int_0^1 y_t(z)^{\frac{\varepsilon-1}{\varepsilon}} dz \right)^{\frac{\varepsilon}{\varepsilon-1}}. \quad (14)$$

Here, $P_t^X(z)$ is the price of the intermediate good produced by firm z in the home country. The problem yields the following intermediate input demand:

$$y_t(z) = \left(\frac{P_t^X(z)}{P_t^X} \right)^{-\varepsilon} y_t. \quad (15)$$

3.3 Intermediate good firms

A continuum of intermediate goods $y_t(z)$ is produced by price setting firms that are optimizing under monopolistic competition. The production function of these firms is a CES aggregator in energy and value added from a Cobb-Douglas bundle of capital and labor, following Hassler et al. (2021):

$$y_t(z) = A_t^Y \left[(1 - \gamma_Y)^{\frac{1}{\varrho_Y}} ((u_t^Y k_{t-1}^Y(z))^{\alpha} (h_t^Y(z))^{1-\alpha})^{\frac{\varrho_Y-1}{\varrho_Y}} + (\gamma_Y)^{\frac{1}{\varrho_Y}} (e_t^Y(z))^{\frac{\varrho_Y-1}{\varrho_Y}} \right]^{\frac{\varrho_Y}{\varrho_Y-1}}, \quad (16)$$

where $e_t^Y(z)$, $u_t^Y k_{t-1}^Y(z)$ and $h_t^Y(z)$ is the energy, effective capital and labor demanded by firm i , respectively. α is the capital share in the value added from capital and labor, γ_Y is the energy share in intermediate goods production and ϱ_Y is the elasticity of substitution between energy and the capital-labor bundle.

Firms set their price P_t^X and choose input factors capital, labor and energy to maximize profits subject to their production technology (16) and the demand of the final good firm (15). Prices are set in Calvo-style staggered contracts, such that each firm faces a constant probability $1 - \theta_P$ of being able to adjust its price. The remaining firms that are not able to reoptimize set their price according to $P_t^X(z) = P_{t-1}^X(z)\pi$. The optimal price-setting problem is derived in Appendix C.2.

3.4 Energy sector

A representative energy firm combines two different energy sources, green energy e_t^G and fossil energy e_t^F , to provide energy services to households and for intermediate goods production. The energy inputs are bundled using the following CES aggregator:

$$e_t = \left((1 - \zeta)^{\frac{1}{\xi}} (e_t^G)^{\frac{\xi-1}{\xi}} + \zeta^{\frac{1}{\xi}} (e_t^F (1 - \Gamma_t))^{\frac{\xi-1}{\xi}} \right)^{\frac{\xi}{\xi-1}}, \quad (17)$$

where ξ is the elasticity of substitution between green and fossil energy and ζ determines the share of fossil energy in energy production. The energy firm faces quadratic adjustment costs Γ_t in fossil energy, defined as:

$$\Gamma_t = \frac{\kappa_E}{2} \left(\frac{e_t^F}{e_{t-1}^F} - 1 \right)^2. \quad (18)$$

These costs are specified analogously to investment adjustment costs in Christiano et al. (2005) and are crucial for capturing the gradual adjustment of fossil energy use following a carbon price increase. Such frictions may reflect long-term supply contracts with fossil fuel providers or limited infrastructure to substitute toward renewable energy sources.

Energy firm profits are defined as follows:

$$\Pi_t^E = p_t^E e_t - p_t^F (1 + \tau_t) e_t^F - p_t^G e_t^G, \quad (19)$$

where the carbon policy rate τ_t is modeled as a surcharge on the price of fossil energy. This implies a trade-off for energy firms. Higher carbon prices create an incentive for energy firms to reduce fossil fuel use to lower production costs. However, the firms face adjustment costs, preventing large and abrupt cuts in fossil energy use. I model carbon policy as a carbon tax for simplicity, because both carbon taxes and cap-and-trade systems like the EU ETS increase the price of fossil fuel use to reduce emissions. I assume that the carbon tax rate follows an AR(1) process:

$$\log(\tau_t) = (1 - \rho_\tau) \log(\bar{\tau}) + \rho_\tau \log(\tau_{t-1}) + \epsilon_t^\tau, \quad (20)$$

where ϵ_t^τ is an exogenous carbon price shock and $\bar{\tau}$ is the steady state carbon tax rate.

The energy firm maximizes profits subject to equation 17. The resulting demand equations for fossil and green energy are given by:

$$e_t^F = \zeta \left(\frac{(1 + \tau_t) p_t^F}{(1 - \Gamma_t - \Gamma'_t e_t^F) p_t^E} \right)^{-\xi} \frac{e_t}{1 - \Gamma_t}, \quad (21)$$

$$e_t^G = (1 - \zeta) \left(\frac{p_t^G}{p_t^E} \right)^{-\xi} e_t, \quad (22)$$

Both energy inputs are produced using a Cobb-Douglas bundle of sector-specific capital and labor services k_t^j and h_t^j , $j \in \{F, G\}$:

$$e_t^j = A_t^j (u_t^j k_{t-1}^j)^\alpha (h_t^j)^{1-\alpha}, \quad j \in \{F, G\}, \quad (23)$$

where u_t^j is the sector-specific rate of capacity utilization.

Fossil energy production generates carbon emissions m_t , such that:

$$m_t = \vartheta e_t^F, \quad (24)$$

where ϑ determines the carbon content of fossil energy production.

3.5 Climate change

Following Golosov et al. (2014), I introduce a climate change externality into my model to capture negative effects of increasing atmospheric carbon on the economy. The externality creates a two-way interaction between the economy and climate change. In the benchmark model, fossil energy production generates carbon emissions, which feed into the stock of atmospheric carbon. The stock of atmospheric carbon evolves according

to the following process:

$$S_t = (1 - \delta_S)S_{t-1} + (m_t + m^{row}), \quad (25)$$

where δ_S is the depreciation rate of carbon dioxide from the atmosphere. The global stock of atmospheric carbon is fueled by domestic euro area emissions m_t and emissions from the rest of the world m^{row} , which, for simplicity, is constant over time.

The model now contains a negative feedback effect from environmental damage due to higher atmospheric carbon on total factor productivity.². Following Golosov et al. (2014), total factor productivity A_t^j in each production sector is then modeled as follows:

$$A_t^j = e^{-\psi_D S_t}, \quad j \in \{Y, G, B\}, \quad (26)$$

where ψ_D is the damage parameter that determines the size of the externality.

3.6 Monetary and fiscal policy

The fiscal authority levies the carbon tax on energy firms and rebates the revenues to Ricardian households through lump-sum transfers. This provides a useful benchmark for revenue use, consistent with the EU ETS, where revenues are intended either to be returned to households or to finance environmental projects, with allocation left to the discretion of member states. I abstract from the existence of public debt and assume the fiscal authority runs a balanced budget at all times. The government budget constraint takes the following form:

$$\tau_t p_t^B e_t^B = T_t + g, \quad (27)$$

where government spending g is assumed to be constant.

The central bank follows a Taylor rule to set the nominal interest rate r_t :

$$\frac{r_t}{r} = \left(\frac{r_{t-1}}{r} \right)^{\rho_r} \left[\left(\frac{\pi_t}{\pi} \right)^{\phi_\pi} \left(\frac{gdp_t}{gdp} \right)^{\phi_y} \right]^{(1-\rho_r)}, \quad (28)$$

In the baseline analysis, the central bank is assumed to respond to headline HICP inflation and real GDP. Since the distinction between output and the output gap may matter for monetary policy design, I examine whether potential output reacts to carbon price shocks. Re-running the local projections from Section 2 for potential output and the output gap shows no significant response of potential output to the carbon price shock. As shown

²An alternative approach in other environmental DSGE models is to include the pollution externality directly into the utility function of households (see Acemoglu et al. (2012), Benmir et al. (2020), Barrage (2020)). However, Nordhaus (2008) and Heutel (2012) argue that such a modeling choice would be more appropriate for conventional pollutants that directly affect health rather than greenhouse gases.

in Figure B.4 in the Appendix, potential output remains broadly unchanged, while real GDP and the output gap exhibit similar dynamics in both direction and magnitude. This suggests that using real GDP directly, rather than an output gap relative to potential output, provides a reasonable and empirically consistent approximation in the Taylor rule specification³.

3.7 Market clearing and functional forms

The labor and energy market clear such that:

$$h_t = h_t^Y + h_t^F + h_t^G, \quad (29)$$

$$e_t = \lambda c_{t,H}^E + (1 - \lambda) c_{t,R}^E + e_t^Y. \quad (30)$$

Aggregate investment is defined as follows:

$$i_t = i_t^Y + i_t^F + i_t^G. \quad (31)$$

Aggregating firm profits implies:

$$\Pi_t = \Pi_t^Y + \Pi_t^E + \Pi_t^F + \Pi_t^G. \quad (32)$$

The resource constraint of the economy is then obtained by plugging the government budget constraint and the profit functions of intermediate goods firms and energy producers into the weighted sum of household budget constraints:

$$y_t = c_t^X + i_t + g + \sum_j a(u_t^j) k_{t-1}^j, \quad j \in \{Y, B, G\}. \quad (33)$$

Real GDP is measured as follows:

$$gdp_t = y_t + p_t^E c_t^E = p_t c_t + i_t + g, \quad (34)$$

where aggregate consumption expenditure is defined as:

$$p_t c_t = \lambda p_{t,H} c_{t,H} + (1 - \lambda) p_{t,R} c_{t,R}. \quad (35)$$

³Potential output data are taken from the OECD Economic Outlook database. The OECD defines potential output as the level of GDP consistent with stable inflation, derived from a production function approach that estimates trend total factor productivity, structural unemployment, and capital accumulation. While this concept differs from the flexible-price, flexible-wage potential output in New Keynesian models, it provides a useful benchmark for assessing the behavior of potential output in the data.

The capacity utilization adjustment cost function is defined as:

$$a(u_t) = \frac{1}{2}\sigma_0\sigma_a u_t^2 + \sigma_0(1 - \sigma_a)u_t + \sigma_0 \left(\frac{1}{2}\sigma_a - 1 \right), \quad (36)$$

where σ_0 is set such that $a(1) = a'(1) = 0$ in steady state. The parameter σ_a controls the curvature of the adjustment cost function, such that a higher σ_a implies larger costs when changing capacity utilization.

A full set of equilibrium equations as well as the steady state of the model is listed in Appendix C.3.

4 Estimation Results

I estimate the key parameters of the model by matching the dynamic responses to a carbon price shock in the model with the estimated impulse responses from the data presented in section 2 using Bayesian impulse response matching. First, I calibrate a set of parameters and then estimate the remaining parameters conditional on the set of calibrated parameters.

4.1 Estimation methodology

For the estimation I follow the limited information Bayesian methodology developed in Christiano et al. (2010) that minimizes the distance between the dynamic impulse responses to the carbon price shock ϵ_t^τ in the model and the analog responses in the data. The impulse responses from the data are estimated using local projections in section 2. I the following variables from the local projections for the estimation procedure: energy inflation, headline inflation, real fossil energy prices, GHG emissions, policy rate, real GDP, real consumption, real investment, real wages and capacity utilization.

Following Christiano et al. (2010), the estimation procedure relies on the assumption that the structural model correctly describes the data-generating process. Let θ_0 denote the true values of the model parameters, and let $\psi(\theta)$ represent the mapping from the parameter space to the model-implied impulse responses. Then, $\psi(\theta_0)$ corresponds to the true impulse responses, which are estimated from the data as $\hat{\psi}$. Under standard asymptotic sampling theory, when the number of observations T is large, the empirical impulse responses satisfy:

$$\sqrt{T} \left(\hat{\psi} - \psi(\theta_0) \right) \xrightarrow{d} N(0, W(\theta_0, \zeta_0)). \quad (37)$$

Here, θ_0 represents the true values of the model parameters, while ζ_0 denotes the true values of shocks that are not explicitly estimated. The $N \times 1$ vector $\hat{\psi}$ includes the contemporaneous and 11 lagged responses of the 10 variables used for the estimation.

The asymptotic distribution of $\hat{\psi}$ can be rewritten as:

$$\hat{\psi} \xrightarrow{d} N(\psi(\theta_0), V), \quad (38)$$

where $V = W(\theta_0, \zeta_0)/T$. In practice, I use a consistent estimator for V , considering only diagonal elements, as suggested by Christiano et al. (2010).

To estimate the model parameters, I treat $\hat{\psi}$ as observed data and specify prior distributions for θ . Using Bayes' theorem, I compute the posterior distribution of θ given $\hat{\psi}$ and V . The likelihood function for $\hat{\psi}$ given θ is approximated by:

$$f(\hat{\psi}|\theta, V) = (2\pi)^{-N/2}|V|^{-1/2} \exp \left[-0.5(\hat{\psi} - \psi(\theta))'V^{-1}(\hat{\psi} - \psi(\theta)) \right]. \quad (39)$$

Maximizing this function provides an approximate maximum likelihood estimator for θ . The likelihood function is derived from the asymptotic distribution of the impulse responses and accounts for estimation uncertainty. I obtain parameter estimates by maximizing the posterior density and use a Markov Chain Monte Carlo (MCMC) algorithm to sample from the posterior distribution.

4.2 Calibrated parameters

The model is calibrated to the euro area at a quarterly frequency. All calibrated parameter values are shown in Table 1.

Table 1: Calibrated parameters

Parameter	Description	Value	Source
$\omega_{e,c}^R$	Energy share in consumption R	0.07	Eurostat, HFCS (2015)
$\omega_{e,c}^H$	Energy share in consumption H	0.16	Eurostat, HFCS (2015)
$\omega_{e,y}$	Energy share in production	0.07	Coenen et al. (2024)
ζ	Green energy share	0.15	Eurostat
π	Gross st.-st. inflation rate	1.005	ECB target, annual rate 2%
β	Discount factor	0.995	Annual real rate 2%
φ	Inverse Frisch elasticity	1	Literature
α	Capital share in production	0.3	Literature
δ	Depreciation rate	0.025	Literature
μ_P	Gross st.-st. price mark-up	1.2	Literature
μ_W	Gross st.-st. wage mark-up	1.2	Literature
g	Government spending	0.42	Implied by $g/gdp=0.2$
δ_S	Decay atmospheric carbon	0.9983	Hassler et al. (2020)
ϑ	Carbon content of fossil energy	1	Hassler et al. (2020)
$100 \cdot \psi_D$	Damage coefficient	0.002698	Hassler et al. (2020)

The quarterly discount factor is set to $\beta = 0.995$, which implies an annual steady-state real interest rate of 2%. The steady-state inflation rate is calibrated to match an annual

inflation of 2% for both core and headline inflation. The substitution elasticity between intermediate goods is set to $\varepsilon = 6$, which is a standard value in New Keynesian models, implying a gross steady-state price mark-up of $\mu_P = \frac{\varepsilon}{\varepsilon-1} = 1.2$. The gross steady-state wage mark-up is also set to $\mu_W = 1.2$. The capital share in production is set to $\alpha = 0.3$ and capital depreciates at a rate of $\delta = 2.5\%$ each quarter. The inverse Frisch elasticity is set to $\varphi = 1$. Government spending is calibrated to match the euro area government spending to GDP ratio of about 20%.

The energy-related parameters are calibrated to match euro area data in steady state. The share of energy in the consumption bundle, $\omega_{e,c}^i$ for $i \in R, H$, is set to replicate households' energy expenditure shares in the euro area. According to Eurostat, these shares are about 16 percent for households in the bottom income quartile and 7 percent for the remaining households. This calibration implies an economy-wide average energy expenditure share of roughly 9 percent, which is consistent with the HICP weight for energy. The distribution parameter $\gamma_{c,i}$ is then calibrated to ensure this expenditure share for every value of p^E and ϱ_c in steady state:

$$\gamma_{c,j} = \omega_{e,c}^i \left(\frac{p^E}{p_i} \right)^{\varrho_c - 1}, \quad i \in \{R, H\}. \quad (40)$$

Similarly, $\omega_{e,y}$ matches the share of energy in production of about 7% in the euro area following Coenen et al. (2024), such that:

$$\gamma_c = \omega_{e,y} (p^E)^{\varrho_y - 1}. \quad (41)$$

The steady-state share of green energy in aggregate energy production is set to $\zeta = 0.15$, reflecting the average value for the euro area for the sample period of 1999 to 2019.

Finally, for the calibration of the climate module, I use the estimates from Hassler et al. (2020). The damage function coefficient ψ_D is estimated to specifically capture damages from carbon-induced temperature increases in Europe.

4.3 Estimated parameters and results

Conditional on the calibrated parameters, I then estimate the remaining fifteen model parameters. Table 2 reports the prior and posterior distributions of the estimated parameters. This section discusses the estimated parameter values and their implications, with a particular focus on the energy-related parameters.

First, the results imply strong complementarity between energy and other inputs in production as well as energy and non-energy goods in consumption. This complementarity is a standard assumption in macro climate models with energy with values usually ranging between 0.2 and 0.5 (Hassler et al. (2021), Coenen et al. (2024), Diluiso et al. (2021)). My estimates are lie slightly below this range with $\varrho_c = 0.12$ and $\varrho_y = 0.07$.

Table 2: Priors and Posteriors of Parameters

Parameter	Prior	Posterior	
	\mathcal{D} , Mode [5-95%]	Mode	[5-95%]
Energy complementarity firms, ϱ_y	\mathcal{G} , 0.32 [0.13 1.07]	0.07	[0.01 0.17]
Energy complementarity households, ϱ_c	\mathcal{G} , 0.32 [0.13 1.07]	0.12	[0.04 0.27]
Substitution green and fossil energy, ξ	\mathcal{U} , — [0.20 3.80]	0.38	[0.23 0.67]
Fossil energy adjustment cost, κ_E	\mathcal{U} , — [1.50 28.5]	10.1	[6.42 16.3]
Share of Hand-to-Mouth households, λ	\mathcal{B} , 0.28 [0.15 0.48]	0.29	[0.21 0.46]
Habit persistence, b	\mathcal{B} , 0.63 [0.34 0.83]	0.73	[0.43 0.86]
Calvo wage stickiness, θ_w	\mathcal{B} , 0.76 [0.43 0.92]	0.88	[0.72 0.97]
Investment adjustment costs, κ_I	\mathcal{G} , 3.20 [1.27 10.7]	4.26	[0.65 8.73]
Capacity utilization adj. costs, σ_a	\mathcal{G} , 0.44 [0.15 2.46]	0.22	[0.03 1.02]
Calvo price stickiness, θ_p	\mathcal{B} , 0.76 [0.43 0.92]	0.61	[0.36 0.81]
Taylor rule inflation coeff., ϕ_π	\mathcal{G} , 1.58 [1.36 1.84]	1.53	[1.25 1.88]
Taylor rule output coeff., ϕ_y	\mathcal{G} , 0.04 [0.01 0.26]	0.04	[0.00 0.15]
Interest rate smoothing, ρ_r	\mathcal{B} , 0.85 [0.61 0.94]	0.95	[0.90 0.99]
Autocorr. carbon price shock, ρ_τ	\mathcal{B} , 0.84 [0.56 0.95]	0.90	[0.84 0.94]
Std. Dev. carbon price shock, σ_τ	\mathcal{IG} , 0.07 [0.04 0.56]	0.26	[0.21 0.35]
Log marginal likelihood		139.7	

Notes: Posterior mode and intervals are based on a standard MCMC algorithm with 500,000 draws (5 chains, 25% burn-in, acceptance rate about 29%). $\mathcal{B}, \mathcal{G}, \mathcal{U}, \mathcal{IG}$ denote beta, gamma, uniform and inverse-gamma distributions, respectively.

The 90% interval is also on the lower end of estimates in the literature. Such a high degree of complementarity makes households and firms very vulnerable to carbon price shocks, because the sharp increase in energy prices will increase their energy bills, leading to a significant drop in consumption and investment expenditure. These results are in line with Gagliardone and Gertler (2023) who estimate strong complementarities of oil in production and consumption using an oil price shock.

Second, the posterior mode of the substitution elasticity between green and fossil energy is estimated at $\xi = 0.38$. Since this value is well below unity, it implies that green and fossil energy behave as complements rather than substitutes in aggregate energy production. The 90% confidence interval places an upper bound at 0.72, reinforcing the conclusion that the two inputs are complements. Standard values in the literature typically range from 1.8 to 3, suggesting much higher substitutability (Papageorgiou et al. (2017), Coenen et al. (2024)). The relatively low estimate obtained here reflects that the identification strategy captures a short-term substitution elasticity following temporary carbon price shocks, rather than long-term adjustment dynamics in response to permanent carbon price increases. The substitution elasticity remains a key parameter for assessing the effectiveness of carbon pricing policies.

Third, the posterior mode of the fossil energy adjustment cost parameter is signif-

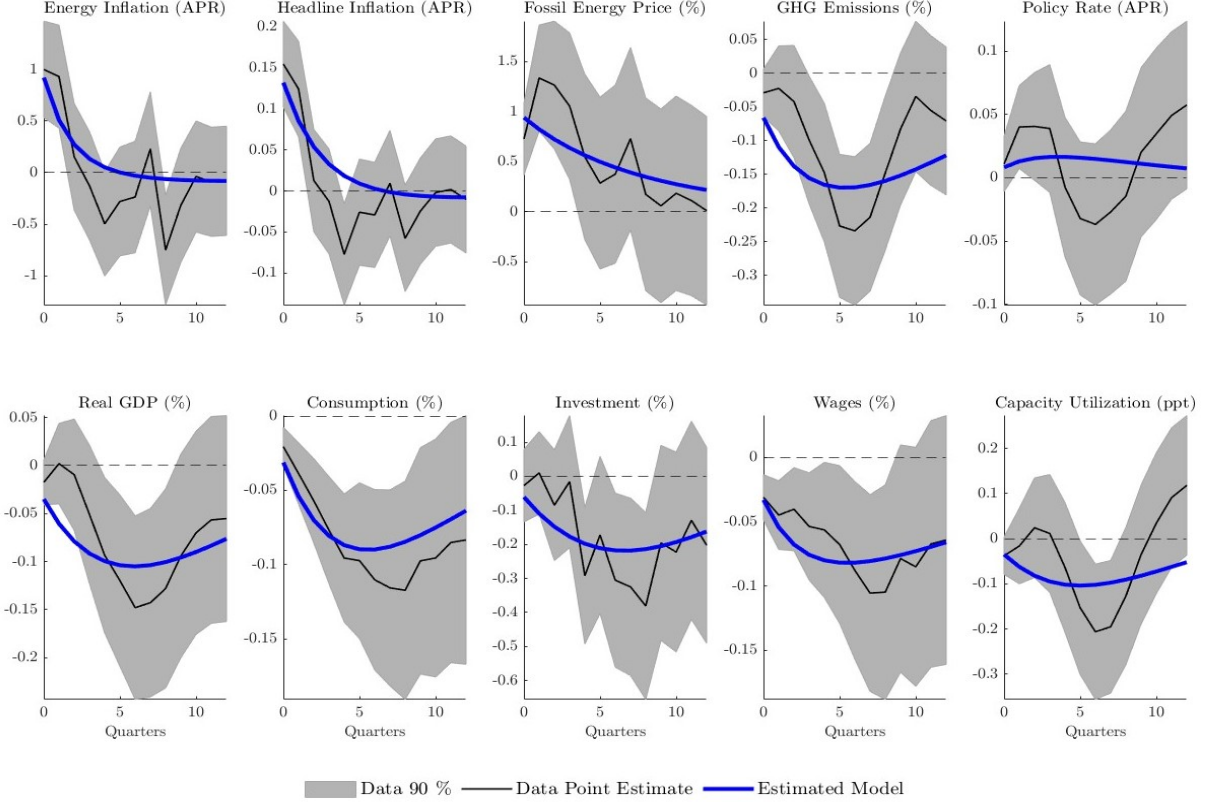


Figure 3: Impulse responses to carbon price shock: Model vs. Data

icantly positive with $\kappa_E = 10.1$. These types of adjustment costs are non-standard in New Keynesian climate models, implying a value of $\kappa_E = 0$. My results suggest that including adjustment costs in the share of fossil energy is crucial to match the lagged response of emissions following an increase in the carbon price. Section 4.4 provides a detailed analysis of the implications of the parameter estimates for ξ and κ_E .

Finally, the estimated posterior mode of the population share of Hand-to-Mouth households is $\lambda = 0.29$. This indicates that accounting for Hand-to-Mouth households is important in order to match the observed response of the economy to the shock. The estimate is also consistent with previous findings for the euro area, such as Dossche et al. (2021) and Almgren et al. (2022).

The remaining parameters, that are not directly related to the energy sector, fall within a reasonable range for standard macroeconomic models. The degree of price stickiness suggests that prices are adjusted every three quarters on average, while nominal wages remain unchanged for about eight quarters on average. Habit persistence $b = 0.73$ is slightly higher, but still close to the estimate of the New Area Wide Model (Coenen et al. (2018), henceforth NAWM II). Investment and capacity utilization adjustment costs are a little lower than suggested by the NAWM II. The estimated Taylor rule coefficients suggest a high degree of interest rate smoothing, while the output gap coefficient is close to zero, which is also in line with the NAWM II. The Taylor rule inflation coefficient is

approximately $\phi_\pi = 1.5$. The persistence of the carbon price shock is $\rho_\tau = 0.9$.

Table 2 indicates that the key energy-related parameters are well identified by the impulse-response matching procedure. The posterior distributions of the substitution elasticity between green and fossil energy (ξ), the fossil energy adjustment cost (κ_E), and the energy complementarity parameters (φ_y, φ_c) are substantially more concentrated than their priors and shift toward values that improve the model's ability to match the empirical impulse responses. Although the macro data provide weaker identification for the share of Hand-to-Mouth households (λ), this parameter is crucial for reproducing the observed consumption dynamics. Section 4.4 discusses its role in more detail. Several remaining parameters, such as wage stickiness (θ_w) and habit formation (b), are also reasonably well identified, with posterior intervals narrowing relative to the prior. In contrast, the Taylor rule coefficients (ϕ_π, ϕ_y) remain only weakly informed by the data, consistent with the empirically muted response of the policy rate to carbon price shocks. However, the interest rate smoothing parameter (ρ_r) is tightly estimated and concentrated near one.

Figure 3 compares the dynamic impulse responses from the model, depicted by the blue line, to the responses estimated from the data in section 2, depicted by the black line. The grey areas are the 90% confidence intervals from the local projections. The model successfully replicates the key dynamics observed in the data following a carbon price shock. Since aggregate energy prices are a bundle of fossil and green energy prices, an increase in the carbon price triggers a surge in energy inflation. This, in turn, raises headline inflation both directly through higher household energy expenditures, and indirectly, as firms pass on increased production costs to consumers. Higher energy bills immediately reduce consumption and investment, while rising production costs cause firms to cut wages and capacity utilization. The resulting decline in labor income further depresses aggregate demand. These demand-side effects are amplified by an increase in real interest rates as monetary policy responds to inflationary pressures. Finally, higher fossil energy prices induce energy producers to gradually reduce fossil energy use, leading to a persistent decline in emissions.

4.4 Counterfactual analysis

This section examines the role of three key parameters: the substitution elasticity between green and fossil energy (ξ), the fossil energy adjustment cost parameter (κ_E), and the share of Hand-to-Mouth agents (λ). The first two parameters determine how flexibly firms and households can adjust their energy use and how smoothly the economy transitions away from fossil fuels in response to policy changes, while λ governs the share of the population that is particularly vulnerable to energy price increases. To illustrate how these parameters shape model dynamics, I fix all estimated parameters at their

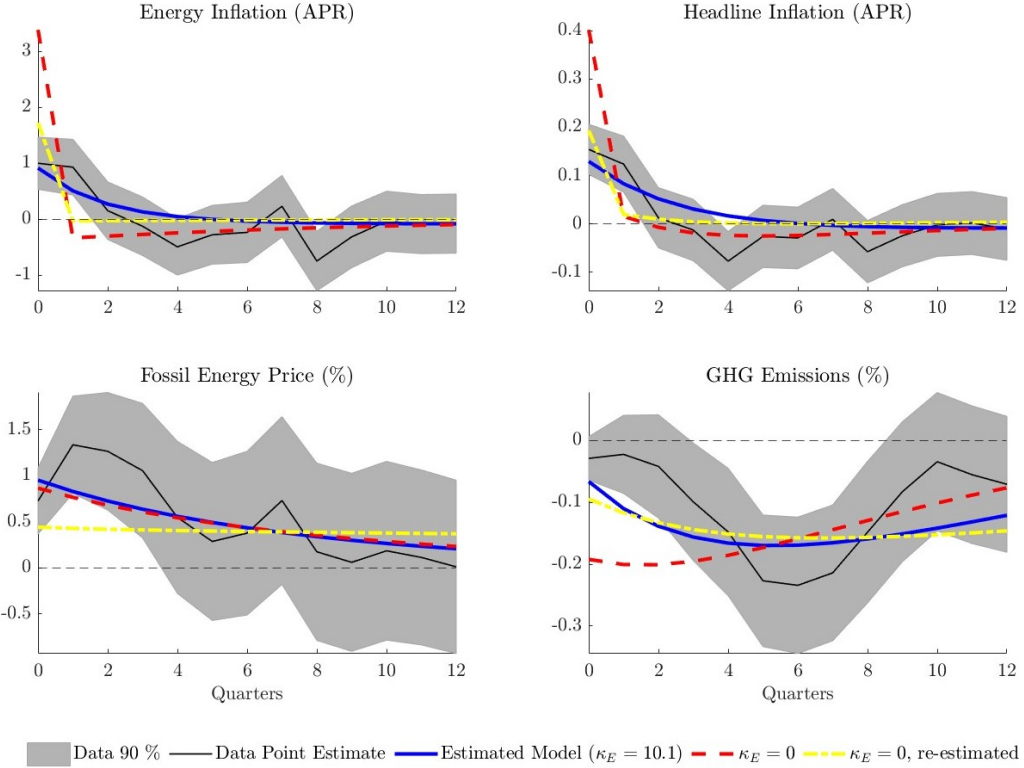


Figure 4: Impulse responses to carbon price shock: Baseline ($\kappa_E = 10.1$) vs. $\kappa_E = 0$

posterior modes (as reported in Table 2) and simulate three counterfactual scenarios: (i) no fossil energy adjustment costs ($\kappa_E = 0$), (ii) higher substitutability between green and fossil energy ($\xi = 3$), and (iii) a representative-agent economy ($\lambda = 0$). I then re-estimate the model under each counterfactual, keeping all other parameters unchanged, and compare the resulting impulse responses to the baseline estimates shown in Figure 3. Note that I focus on a subset of variables from the estimation that are most relevant for the respective parameter. The full set of counterfactual impulse responses is provided in Appendix D.

Figure 4 illustrates scenario (i), which sets the fossil energy adjustment cost parameter to $\kappa_E = 0$. The strongest effect appears in aggregate energy prices: energy inflation spikes by more than 3 percentage points on impact, which is over three times the response observed in the data. This surge quickly feeds through to headline inflation, which rises by around 0.4 percentage points, amplifying short-run cost pressures across the economy. Because energy firms can immediately substitute away from fossil energy use in this scenario, emissions fall sharply on impact. As a result, the model fails to capture the gradual and persistent decline in emissions observed in the data. In practice, adjustment frictions such as infrastructure limitations, supply constraints, and technology adoption barriers slow the transition away from fossil fuels, dampening the short-run response. Re-estimating the model without fossil energy adjustment costs yields inflation responses closer to the data. However, matching the gradual decline in emissions requires assuming

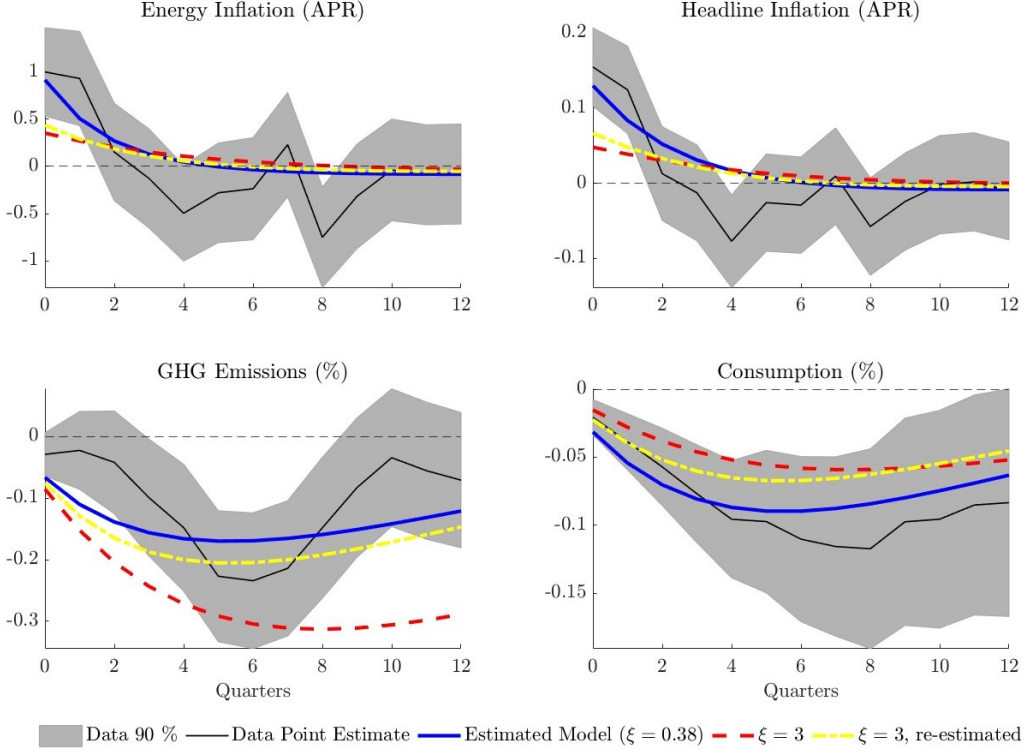


Figure 5: Impulse responses to carbon price shock: Baseline ($\xi = 0.38$) vs. $\xi = 3$

a highly persistent shock ($\rho_\tau = 0.99$), which is reflected in the response of fossil energy prices. The fossil energy price increases by roughly 0.5 percent on impact, which is below the empirical estimate, and remains unchanged for almost three years. The re-estimated model with $\kappa_E = 0$ yields a log marginal likelihood of 118.2, compared to 139.7 for the baseline model, indicating a substantially poorer fit to the data.

Figure 4 illustrates scenario (ii), which sets the substitution elasticity between green and fossil energy to $\xi = 3$. A higher elasticity implies that energy producers can more easily substitute away from fossil energy, which dampens the sharp impact response of aggregate energy inflation. As a result, the rise in headline inflation is substantially muted, alleviating some of the short-run cost pressures on households. This, in turn, leads to a noticeably smaller contraction in consumption compared to the baseline estimated model. At the same time, greater substitutability accelerates the shift toward green energy, producing a stronger and more immediate reduction in emissions than observed in the data. Re-estimating the model with higher substitutability helps match the smaller decline in emissions by implying a less persistent shock ($\rho_\tau = 0.84$), but it still fails to reproduce the initial inflation surge. The slightly better fit of the consumption response is mainly driven by a higher estimated share of Hand-to-Mouth households ($\lambda = 0.4$). The re-estimated model with $\xi = 3$ yields a log marginal likelihood of 126.2, compared to 139.7 for the baseline model, again implying a poorer fit to the data.

Figure D.1 in the Appendix shows that increasing the substitutability between energy

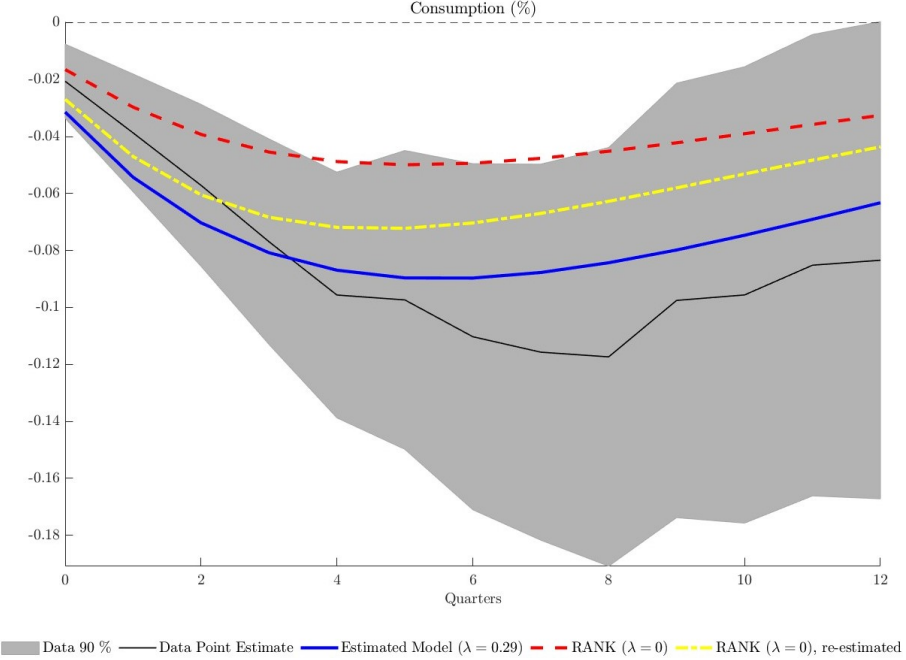


Figure 6: Impulse responses to carbon price shock: Baseline ($\lambda = 0.29$) vs. RANK, $\lambda = 0$

and other inputs or goods in production or consumption yields similar results. When the production function is Cobb–Douglas ($\varrho_y = 1$), intermediate-goods producers can more easily substitute away from energy, reducing their energy demand and mitigating the rise in marginal costs. Likewise, when the household consumption bundle is Cobb–Douglas ($\varrho_c = 1$), households adjust their energy demand more strongly in response to higher energy prices. Overall, as with higher substitutability between green and fossil energy, these parameter settings make the economy less sensitive to carbon price shocks.

Finally, Figure 6 compares the impulse response of consumption in the baseline heterogeneous-agent model to a standard representative-agent New Keynesian (RANK) model where all households are Ricardian. Hand-to-Mouth households spend a relatively larger share of their income on energy than Ricardian agents. In addition, since the H households consume all disposable income in each period, they cannot self-insure against adverse shocks. A model that does not include H households has difficulties reproducing the significant fall in private consumption observed in the data. Re-estimating the model with $\lambda = 0$ improves the fit for consumption by implying a smaller degree of habit formation ($b = 0.63$). However, the log marginal likelihood of 134.3 still suggests a somewhat poorer overall fit than the baseline model, although the difference is less pronounced than in scenarios (i) and (ii).

5 Monetary Policy

While central banks do not directly engage in climate change mitigation, the impact of carbon price shocks on inflation and output means its macroeconomic consequences are relevant for monetary policy. As shown above, a carbon price shock raises inflation while reducing output, creating a monetary policy trade-off. This section examines the Ramsey optimal monetary policy response to a carbon price shock and compares how alternative policy rules shape the transmission of carbon pricing to the macroeconomy.

5.1 Optimal monetary policy

In the optimal monetary policy analysis, the central bank is modeled as a benevolent Ramsey planner that chooses the optimal paths of all endogenous variables under commitment, using the nominal interest rate r_t as its policy instrument to maximize social welfare from a timeless perspective. Social welfare is defined as the population-weighted average of Ricardian and Hand-to-Mouth households' utility:

$$\max \mathcal{W}_0 = \mathbb{E}_0 \sum_{t=0}^{\infty} \beta^t \left[\lambda \mathcal{U}_t^H + (1 - \lambda) \mathcal{U}_t^R \right], \quad (42)$$

subject to the private sector constraints implied by firms' profit maximization and households' utility-maximizing behavior. The planner internalizes nominal price and wage rigidities, which shape the transmission of monetary policy to inflation and real activity. The carbon tax path is exogenous and taken as given by the planner, so environmental policy is not optimal. The central bank is assumed to commit to a contingent policy rule announced at time 0, allowing for dynamic adjustment of the policy instrument to evolving economic conditions. I consider a second-best allocation, following Schmitt-Grohé and Uribe (2004), since the steady state is inefficient due to monopolistic competition in intermediate-good production and wage setting.

Figure 7 compares the Ramsey-optimal monetary policy response to a carbon price shock with the impulse responses under the estimated Taylor rule. The contrast is striking: while the Taylor rule prescribes an increase in the policy rate to contain inflation, the Ramsey planner lowers the rate sharply. This result highlights a key trade-off for monetary policy: stabilizing inflation would require higher interest rates, but this would amplify the contraction in aggregate demand. The planner's response mitigates the decline in output and consumption but comes at the cost of temporarily higher headline and core inflation. In other words, the planner tolerates short-run inflationary pressures to stabilize real activity. This difference in policy responses reflects the structural characteristics of the economy: energy is a critical and hard-to-substitute input in production and consumption. Fossil and green energy are not easily substitutable in energy production,

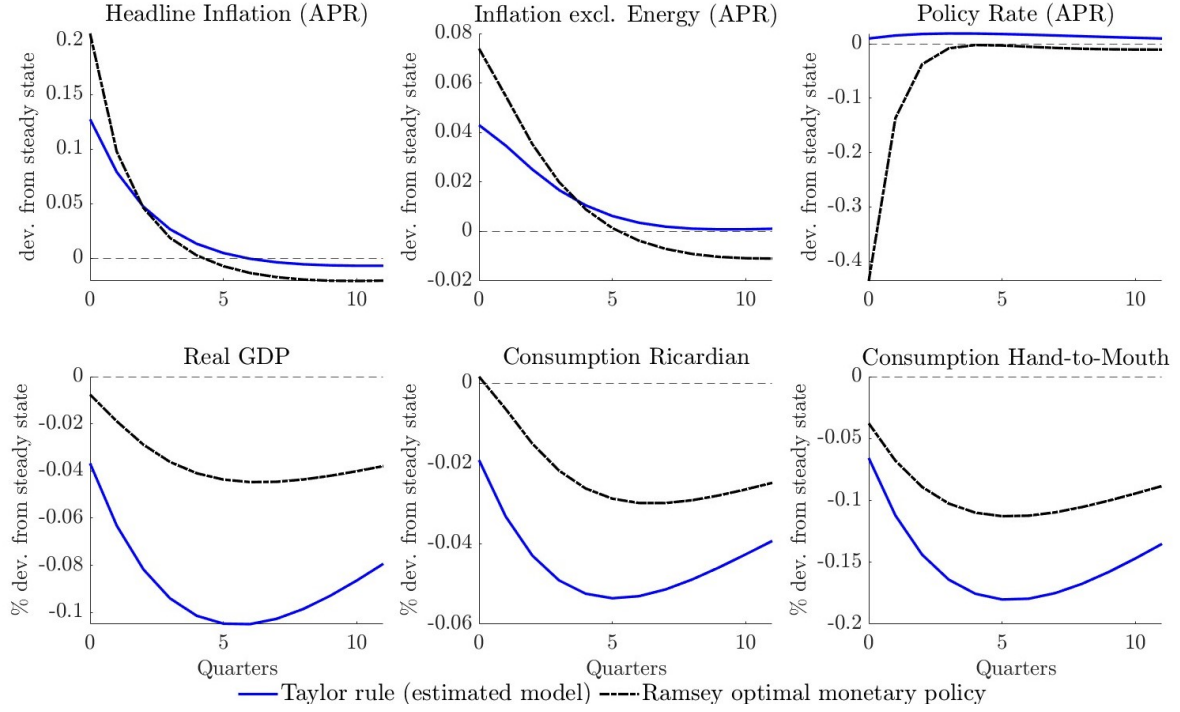


Figure 7: Impulse responses to a carbon price shock: Ramsey optimal monetary policy vs. Taylor rule (estimated model)

energy use is complementary to other production inputs, and households face limited scope to reduce energy consumption. Consequently, higher fossil energy prices raise costs for firms and households, lowering labor demand, wages, and disposable income. In this environment, an aggressive interest rate increase to contain inflation amplifies the fall in demand and leads to larger welfare losses, making an initial rate cut optimal.

The sharp initial interest rate cut is strongly driven by the significant fall in Hand-to-Mouth consumption in response to the carbon price shock. As Hand-to-Mouth households spend a relatively larger fraction of their disposable income on energy and cannot self-insure against adverse shocks, they are hit substantially harder by the shock than Ricardian households. Figure E.1 in the Appendix shows that if the planner only maximizes welfare based on Ricardian households' utility, the interest rate trajectory is much smoother. However, the planner in this scenario still clearly favors output stabilization over inflation stabilization.

To better understand the mechanisms shaping the optimal monetary policy response, Figure 8 presents a set of counterfactual experiments in which key estimated frictions are sequentially removed from the model. Starting from the baseline (black dash-dotted line), I first eliminate Hand-to-Mouth households by setting $\lambda = 0$, yielding a RANK economy shown by the red dashed line. Since liquidity-constrained households are more vulnerable to higher energy costs, their removal from the model dampens the fall in aggregate demand and output. Consequently, the Ramsey planner cuts the policy rate

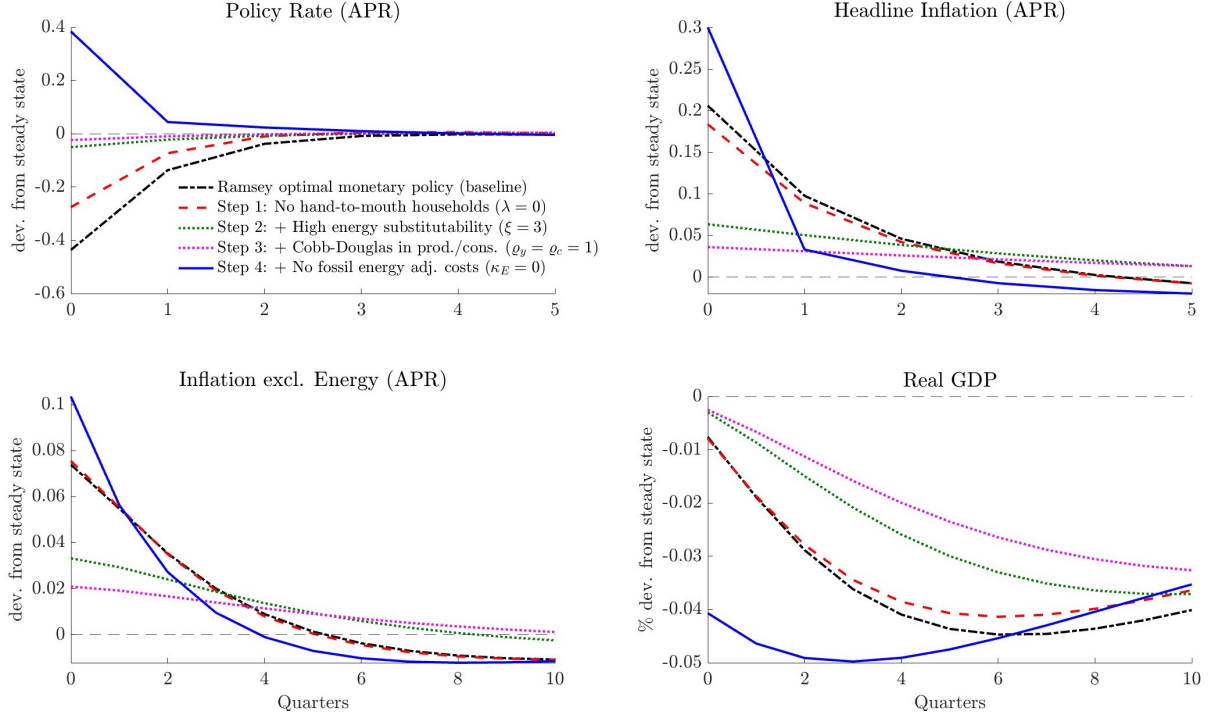


Figure 8: Drivers of the optimal monetary policy response to a carbon price shock

Notes: The figure shows a sequence of counterfactuals removing key model features step by step: (i) RANK ($\lambda = 0$); (ii) higher substitutability between green and fossil energy ($\xi = 3$); (iii) Cobb–Douglas production and consumption ($\varrho_y = \varrho_c = 1$); and (iv) no fossil energy adjustment costs ($\kappa_E = 0$).

less aggressively.

In the next step, depicted by the green dotted line, I increase the substitutability between fossil and green energy to $\xi = 3$. This facilitates adjustment in the energy mix, substantially mitigating the rise in production costs and inflation, and further reduces the need for monetary easing. When I additionally allow for Cobb–Douglas substitution between energy and non-energy goods in both production and consumption ($\varrho_c = 1$, $\varrho_y = 1$), the carbon price shock becomes even less distortionary. Firms and households can now substitute away from energy, which strongly mitigates the effects of the shock on inflation and output, as depicted by the pink dotted line. The optimal interest rate response turns nearly flat, but still falls initially.

Finally, setting the fossil energy adjustment cost to zero ($\kappa_E = 0$) allows an instantaneous shift away from fossil inputs. This generates a short-lived but strong surge in energy inflation, which transmits directly to headline and core inflation, as depicted by the blue solid line. At the same time, the fall in aggregate demand is strongly damped by the parameter settings in the previous steps. The planner therefore raises the policy rate temporarily, resulting in a sharper initial contraction in real GDP. Note that removing adjustment costs alone does not imply a rate hike, as shown in Figure E.2 in the Appendix. In isolation, dropping fossil energy adjustment costs amplifies the initial contraction in aggregate demand, which leads the planner to cut the policy rate even

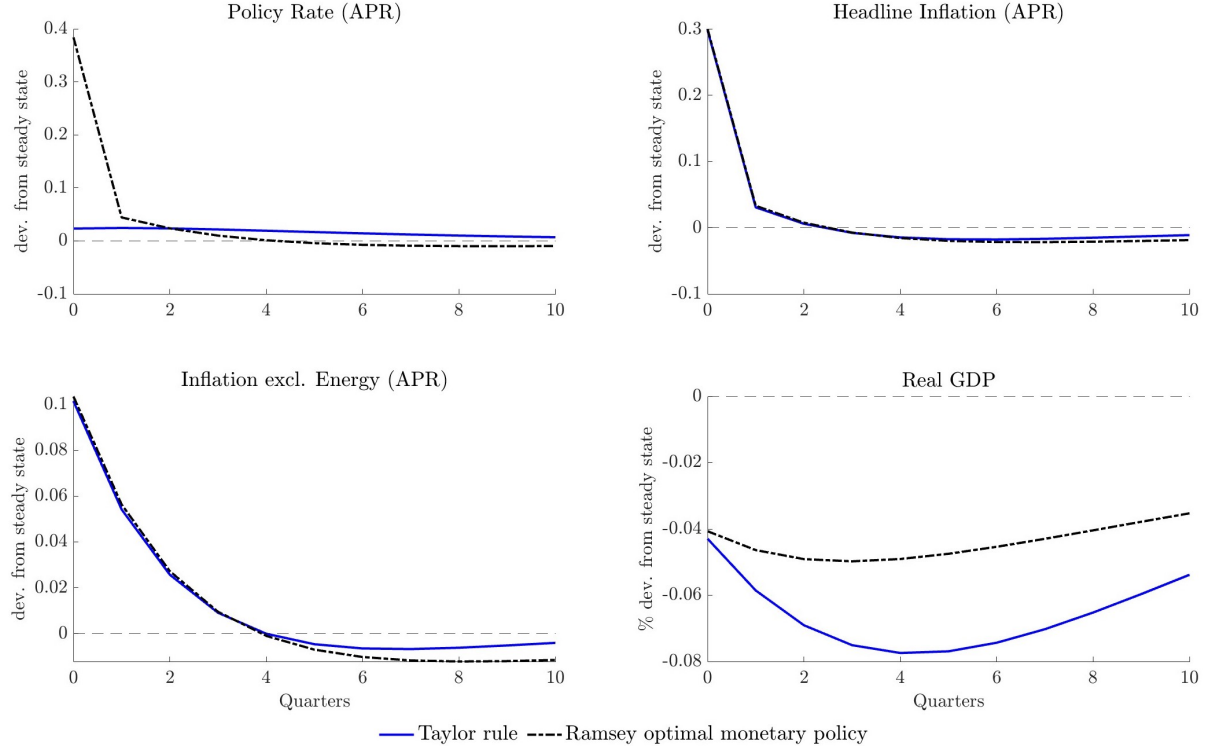


Figure 9: Impulse responses to a carbon price shock in model without key frictions: Ramsey optimal monetary policy vs. Taylor rule

Notes: The figure shows the impulse responses to a carbon price shock in a RANK model ($\lambda = 0$) with higher substitutability between green and fossil energy ($\xi = 3$), Cobb–Douglas production and consumption ($\varrho_y = \varrho_c = 1$), and no fossil energy adjustment costs ($\kappa_E = 0$).

more sharply. Overall, these counterfactual experiments highlight that the combination of energy rigidities, complementarity, and heterogeneity is crucial for obtaining a policy rate cut as the Ramsey optimal monetary policy response to carbon price shocks.

Figure 9 compares the Ramsey optimal monetary policy response with a central bank following Taylor rule in a model with $\lambda = 0$, $\xi = 3$, $\varrho_y = 1$, $\varrho_c = 1$, and $\kappa_E = 0$. All other parameters are kept at their calibrated or estimated values. The optimal policy features a sharp initial increase in the nominal interest rate, followed by a gradual normalization, with the rate slightly declining about one year after the shock. This anticipated reduction helps to cushion aggregate demand and limits the contraction in real GDP. The responses of headline and core inflation are almost identical across both policy specifications, reflecting the dominant role of the rise in energy inflation, which monetary policy cannot directly offset. Compared to the baseline model results in Figure 7, the planner still mitigates the fall in GDP, but not to the extent that it would generate an even stronger inflationary response. Because the demand-side contraction is more muted and the inflationary pressures are stronger under this parameterization, the monetary policy trade-off shifts more toward inflation stabilization relative to Ramsey optimal monetary policy in the estimated model.

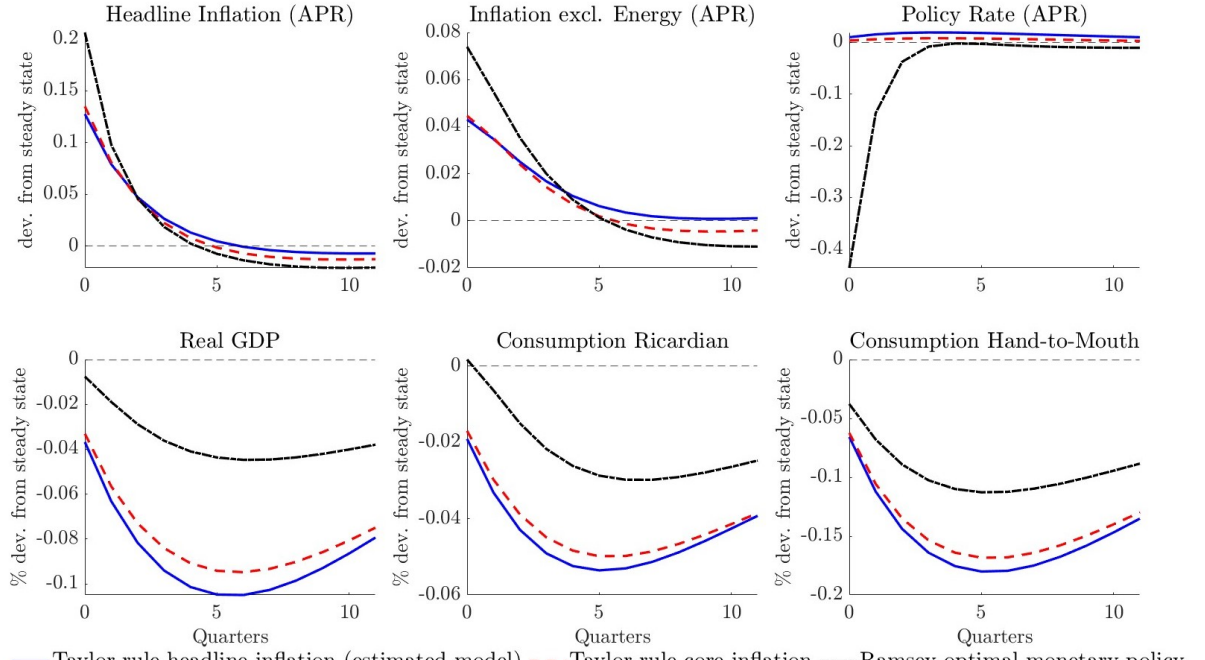


Figure 10: Impulse responses to a carbon price shock: Optimal monetary policy vs. headline inflation stabilization vs. core inflation stabilization

5.2 Alternative Taylor rules

In this section, I analyze the implications of an alternative interest rate rule, more specifically a Taylor rule that focuses on stabilizing core inflation π_t^X instead of headline inflation. The modified Taylor rule is defined as:

$$\frac{r_t}{r} = \left(\frac{r_{t-1}}{r} \right)^{\rho_r} \left[\left(\frac{\pi_t^X}{\pi} \right)^{\phi_\pi} \left(\frac{gdp_t}{gdp} \right)^{\phi_y} \right]^{(1-\rho_r)}. \quad (43)$$

The reaction coefficients ϕ_π , ϕ_y and ρ_r in this specification are the same as in the baseline estimated model.

Figure 10 compares the impulse responses to a carbon price shock when the central follows the modified core inflation Taylor rule to the baseline responses in the estimated model and optimal monetary policy responses. When monetary policy follows a rule that targets core rather than headline inflation, the results come closer to the optimal response. Because core inflation excludes volatile energy prices, the central bank reacts less aggressively to the initial rise in headline inflation. This moderates the rise in real interest rates and thereby the contraction in output and consumption relative to the headline-based rule. While this comes at the cost of a slightly stronger initial increase in headline inflation, this effect is very small. In this sense, a core inflation rule approximates the Ramsey allocation more closely, as it implicitly places less weight on energy-driven price movements and thereby more on stabilizing the real economy, while not strongly increasing inflation volatility.

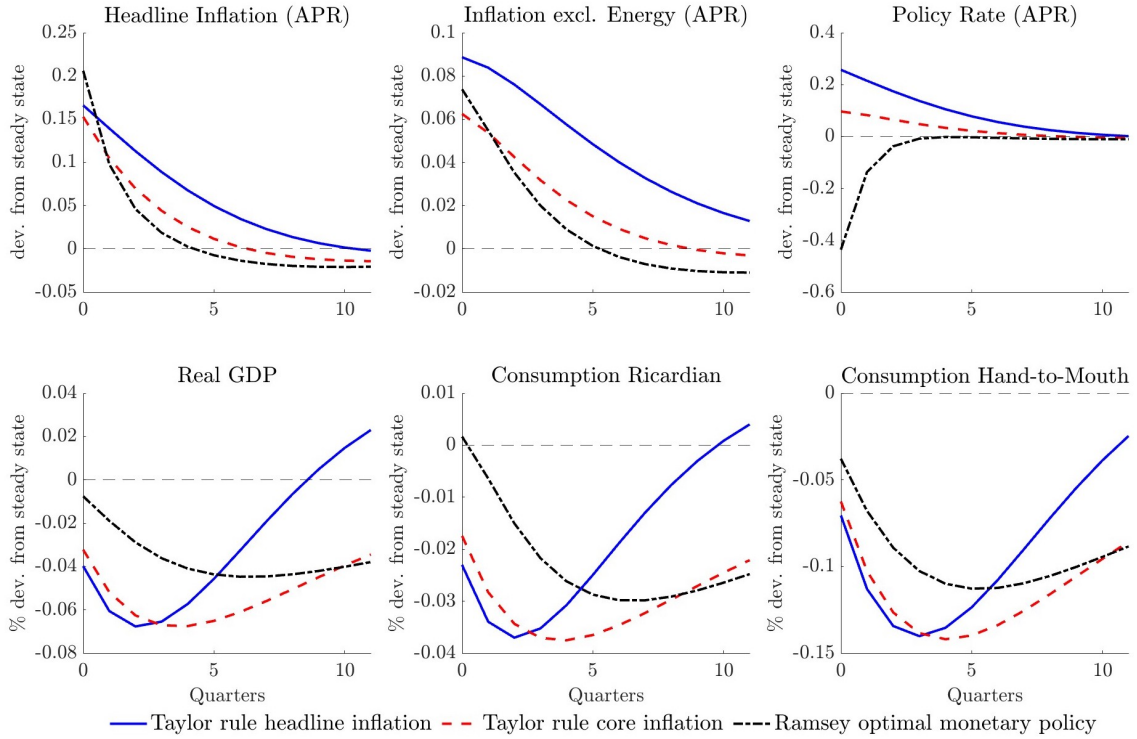


Figure 11: Impulse responses to a carbon price shock: Optimal monetary policy vs. headline inflation stabilization vs. core inflation stabilization without interest rate smoothing in Taylor rules

Notes: The impulse responses for the two Taylor rule scenarios (blue solid and red-dashed line) are generated by setting $\rho_r = 0$. All other model parameters are kept unchanged.

The estimated Taylor rule exhibits substantial interest rate smoothing ($\rho_r = 0.95$), whereas the Ramsey optimal policy responds much more abruptly to the carbon price shock. To assess the role of smoothing, Figure 11 compares the Ramsey response with two alternative Taylor rules in which the smoothing coefficient is set to $\rho_r = 0$. Without smoothing, both Taylor rules imply much stronger rate hikes than in the estimated model. The central bank following a rule that targets headline inflation raises the policy rate sharply on impact, as it reacts to the energy-price-driven increase in headline inflation. This response amplifies the initial fall in consumption and GDP. In contrast, the Taylor rule targeting core inflation generates a noticeably smaller rate increase, because core inflation excludes energy and therefore responds less strongly to the shock. Interestingly, without smoothing, the core inflation rule mitigates both the initial contraction in aggregate demand and the rise in inflation: the resulting paths for headline and core inflation are close to the welfare-optimal Ramsey outcome. After the initial large rate hike, the headline-inflation rule quickly unwinds the increase and returns to steady state after roughly 11 quarters, allowing consumption and GDP to recover faster, but keeping inflation elevated for longer. In contrast, the core inflation rule produces a much flatter interest rate path, keeping demand lower for longer and reducing inflation more persistently.

Overall, these results highlight that monetary policy faces a clear trade-off in responding to carbon price shocks. Monetary policies that mechanically target headline inflation risk exacerbating inefficient output losses, while approaches that give less weight to energy-driven price fluctuations, such as core inflation targeting, deliver outcomes more in line with the welfare-maximizing solution.

6 Conclusion

In this paper, I develop and estimate a heterogeneous-agent New Keynesian macro-climate model that successfully captures the macroeconomic effects of carbon price shocks in the euro area. Using local projections, I document three key empirical responses to carbon price shocks: a gradual decline in emissions, a sharp rise in headline inflation, and a significant drop in economic activity. To account for these dynamics, I identify four model features essential for matching the empirical responses: low substitutability between green and fossil energy, fossil energy adjustment costs, strong complementarity between energy and non-energy goods and inputs in consumption and production, and household heterogeneity. The estimated model closely aligns with the data, providing a robust empirical framework for analyzing the macroeconomic implications of carbon pricing. With this empirically grounded framework, I assess the role of monetary policy in shaping macroeconomic outcomes following carbon price shocks. The results show that a welfare-maximizing Ramsey planner responds to a carbon price shock by lowering the policy rate, prioritizing the stabilization of real activity at the cost of temporarily higher inflation. In the absence of the key model frictions identified in the estimation, however, optimal monetary policy would instead prescribe a rate hike, as inflationary pressures dominate the demand contraction. A central bank that targets core rather than headline inflation can mitigate the GDP losses following a carbon price shock, and is therefore closer to the welfare-optimal policy outcome. These findings contribute to the macro-climate modeling literature by providing a framework that captures the complex interactions between carbon pricing, economic activity, inflation and monetary policy. As carbon pricing is a key instrument of climate policy, such frameworks are essential for designing effective stabilization policies in the green transition.

References

- Acemoglu, Daron, Philippe Aghion, Leonardo Bursztyn, and David Hemous (2012). “The environment and directed technical change”. In: *American economic review* 102.1, pp. 131–166.
- Almgren, Mattias, José-Elías Gallegos, John Kramer, and Ricardo Lima (2022). “Monetary policy and liquidity constraints: Evidence from the euro area”. In: *American Economic Journal: Macroeconomics* 14.4, pp. 309–340.
- Auclert, Adrien, Hugo Monnery, Matthew Rognlie, and Ludwig Straub (2023). *Managing an energy shock: Fiscal and monetary policy*. Tech. rep. National Bureau of Economic Research.
- Barrage, Lint (2020). “Optimal dynamic carbon taxes in a climate–economy model with distortionary fiscal policy”. In: *The Review of Economic Studies* 87.1, pp. 1–39.
- Baumeister, Christiane and James D Hamilton (2019). “Structural interpretation of vector autoregressions with incomplete identification: Revisiting the role of oil supply and demand shocks”. In: *American Economic Review* 109.5, pp. 1873–1910.
- Benmir, Ghassane, Ivan Jaccard, and Gauthier Vermandel (2020). *Green asset pricing*. Tech. rep. ECB Working Paper No. 2477.
- Chan, Jenny, Sebastian Diz, and Derrick Kanngiesser (2024). “Energy prices and household heterogeneity: Monetary policy in a gas-tank”. In: *Journal of Monetary Economics* 147, p. 103620.
- Christiano, Lawrence J, Martin Eichenbaum, and Charles L Evans (2005). “Nominal rigidities and the dynamic effects of a shock to monetary policy”. In: *Journal of political Economy* 113.1, pp. 1–45.
- Christiano, Lawrence J, Mathias Trabandt, and Karl Walentin (2010). “DSGE models for monetary policy analysis”. In: *Handbook of monetary economics*. Vol. 3. Elsevier, pp. 285–367.
- Coenen, Günter, Peter Karadi, Sebastian Schmidt, and Anders Warne (2018). “The New Area-Wide Model II: an extended version of the ECB’s micro-founded model for forecasting and policy analysis with a financial sector”. In.
- Coenen, Günter, Matija Lozej, and Romanos Priftis (2024). “Macroeconomic effects of carbon transition policies: an assessment based on the ECB’s New Area-Wide Model with a disaggregated energy sector”. In: *European Economic Review* 167, p. 104798.
- Del Negro, Marco, Julian Di Giovanni, and Keshav Dogra (2023). “Is the Green Transition Inflationary?” In: *FRB of New York Staff Report* 1053.
- Diluiso, Francesca, Barbara Annicchiarico, Matthias Kalkuhl, and Jan C Minx (2021). “Climate actions and macro-financial stability: The role of central banks”. In: *Journal of Environmental Economics and Management* 110, p. 102548.

- Dossche, Maarten, Jiri Slacalek, and Guido Wolswijk (2021). “Monetary policy and inequality”. In: *Economic Bulletin Articles* 2.
- Erceg, Christopher, Marcin Kolasa, Jesper Lindé, and Andrea Pescatori (2024). “Can Energy Subsidies Help Slay Inflation?” In.
- Gagliardone, Luca and Mark Gertler (2023). “Oil prices, monetary policy and inflation surges”. In.
- Golosov, Mikhail, John Hassler, Per Krusell, and Aleh Tsyvinski (2014). “Optimal taxes on fossil fuel in general equilibrium”. In: *Econometrica* 82.1, pp. 41–88.
- Hassler, John, Per Krusell, and Conny Olovsson (2021). “Directed technical change as a response to natural resource scarcity”. In: *Journal of Political Economy* 129.11, pp. 3039–3072.
- Hassler, John, Per Krusell, Conny Olovsson, and Michael Reiter (2020). “On the effectiveness of climate policies”. In: *IIES WP* 53, p. 54.
- Heutel, Garth (2012). “How should environmental policy respond to business cycles? Optimal policy under persistent productivity shocks”. In: *Review of Economic Dynamics* 15.2, pp. 244–264.
- Jordà, Òscar (2005). “Estimation and inference of impulse responses by local projections”. In: *American economic review* 95.1, pp. 161–182.
- Kängig, Diego R (2021). “The macroeconomic effects of oil supply news: Evidence from OPEC announcements”. In: *American Economic Review* 111.4, pp. 1092–1125.
- (2023). *The unequal economic consequences of carbon pricing*. Tech. rep. National Bureau of Economic Research.
- Konradt, Maximilian and Beatrice Weder di Mauro (2023). “Carbon taxation and greenflation: Evidence from europe and canada”. In: *Journal of the European Economic Association*, jvad020.
- Metcalf, Gilbert E and James H Stock (2023). “The macroeconomic impact of Europe’s carbon taxes”. In: *American Economic Journal: Macroeconomics* 15.3, pp. 265–286.
- Montiel Olea, José Luis and Mikkel Plagborg-Møller (2021). “Local projection inference is simpler and more robust than you think”. In: *Econometrica* 89.4, pp. 1789–1823.
- Nakov, Anton and Carlos Thomas (2023). “Climate-conscious monetary policy”. In.
- Nordhaus, William (2008). *A question of balance: Weighing the options on global warming policies*. Yale University Press.
- Olovsson, Conny and David Vestin (2023). *Greenflation?* Sveriges Riksbank.
- Papageorgiou, Chris, Marianne Saam, and Patrick Schulte (2017). “Substitution between clean and dirty energy inputs: A macroeconomic perspective”. In: *Review of Economics and Statistics* 99.2, pp. 281–290.
- Quilis, Enrique M. (2024). *Temporal Disaggregation*. Accessed: 30 Oct. 2024. URL: <https://de.mathworks.com/matlabcentral/fileexchange/69800-temporal-disaggregation>.

- Sahuc, Jean-Guillaume, Frank Smets, and Gauthier Vermandel (2025). “The New Keynesian Climate Model”. In.
- Schmitt-Grohé, Stephanie and Martin Uribe (2004). *Optimal operational monetary policy in the Christiano-Eichenbaum-Evans model of the US business cycle*.
- Schnabel, Isabel (2022). *A new age of energy inflation: climateflation, fossilflation and greenflation*. Speech by Isabel Schnabel, Member of the Executive Board of the ECB, at a panel on “Monetary Policy and Climate Change” at The ECB and its Watchers XXII Conference. URL: https://www.ecb.europa.eu/press/key/date/2022/html/ecb.sp220317_2~dbb3582f0a.en.html.
- Wu, Jing Cynthia and Fan Dora Xia (2020). “Negative interest rate policy and the yield curve”. In: *Journal of Applied Econometrics* 35.6, pp. 653–672.

A Data sources

The empirical analysis uses euro area data from the following sources:

HICP: Eurostat, table prc_hicp_midx, monthly frequency averaged to convert into quarterly frequency. Specifically, I use the following datasets: *All-items HICP, HICP energy, Overall index excluding energy, HICP gas.*

Real GDP: Eurostat, table namq_10_gdp, quarterly frequency. *Gross domestic product at market prices, chain linked volumes, seasonally and calendar adjusted.*

Real Consumption: Eurostat, table namq_10_gdp, quarterly frequency. *Households and NPISH final consumption expenditure, chain linked volumes, seasonally and calendar adjusted.*

Real Investment: Eurostat, table namq_10_gdp, quarterly frequency. *Gross fixed capital formation, chain linked volumes, seasonally and calendar adjusted.*

Real Wages: Eurostat, table namq_10_gdp, quarterly frequency. *Wages and salaries, current prices, seasonally and calendar adjusted.* Real wages are constructed by deflating nominal wages with the HICP.

Policy rate: ECB MRO rate spliced with shadow rate from Wu and Xia (2020).

GHG emissions: Eurostat, table env_air_gge, quarterly frequency. *Total greenhouse gas emissions, thousand tonnes.*

Energy production: Eurostat, table sts_inpr_q, quarterly frequency. *MIG - energy, production volume index, seasonally and calendar adjusted.*

Capacity Utilization: Eurostat, table ei_bsin_q_r2, quarterly frequency. *Current level of capacity utilization, percent, seasonally and calendar adjusted.*

Brent crude oil price: FRED, table DCOILBRENTEU, daily frequency averaged to convert into quarterly frequency. *Crude Oil Prices: Brent - Europe, Dollars per Barrel.*

Real potential output: OECD Economic Outlook database, quarterly data. *Potential output volume.* The OECD potential output measure is based on a production-function approach that estimates the level of output consistent with stable inflation, accounting for trend labor, capital, and total factor productivity.

Output gap: OECD Economic Outlook database, quarterly data. *Output gap as a percentage of potential GDP.*

Population: Eurostat, table namq_10_pe, quarterly frequency. *Total population, thousand persons, seasonally and calendar adjusted.* Used to express variables in per-capita terms.

B Empirical analysis: Additional figures

B.1 Distribution of carbon price shocks

Figure B.1 shows the time series and distribution of the standardized carbon price shocks from Käenzig (2023), aggregated to quarterly frequency. The red dashed line indicates the magnitude of the shock used in the local projections, i.e. the shock that increases annualized energy inflation by one percentage point on impact.

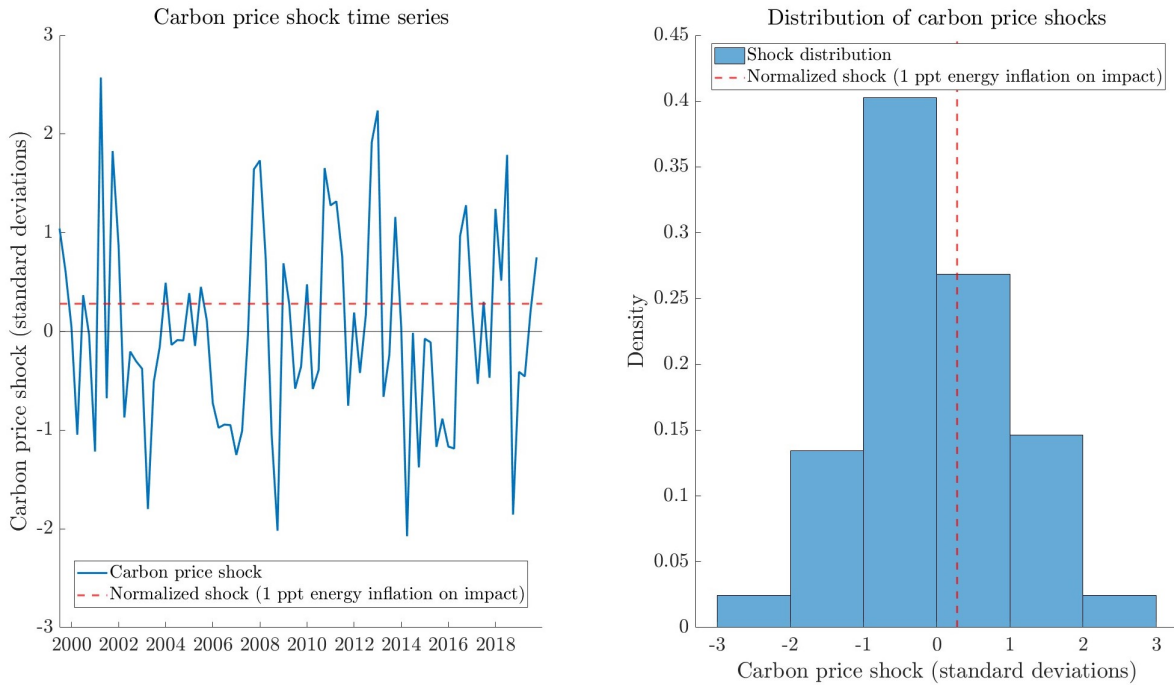


Figure B.1: Carbon price shock time series and distribution

B.2 Local projections: Robustness

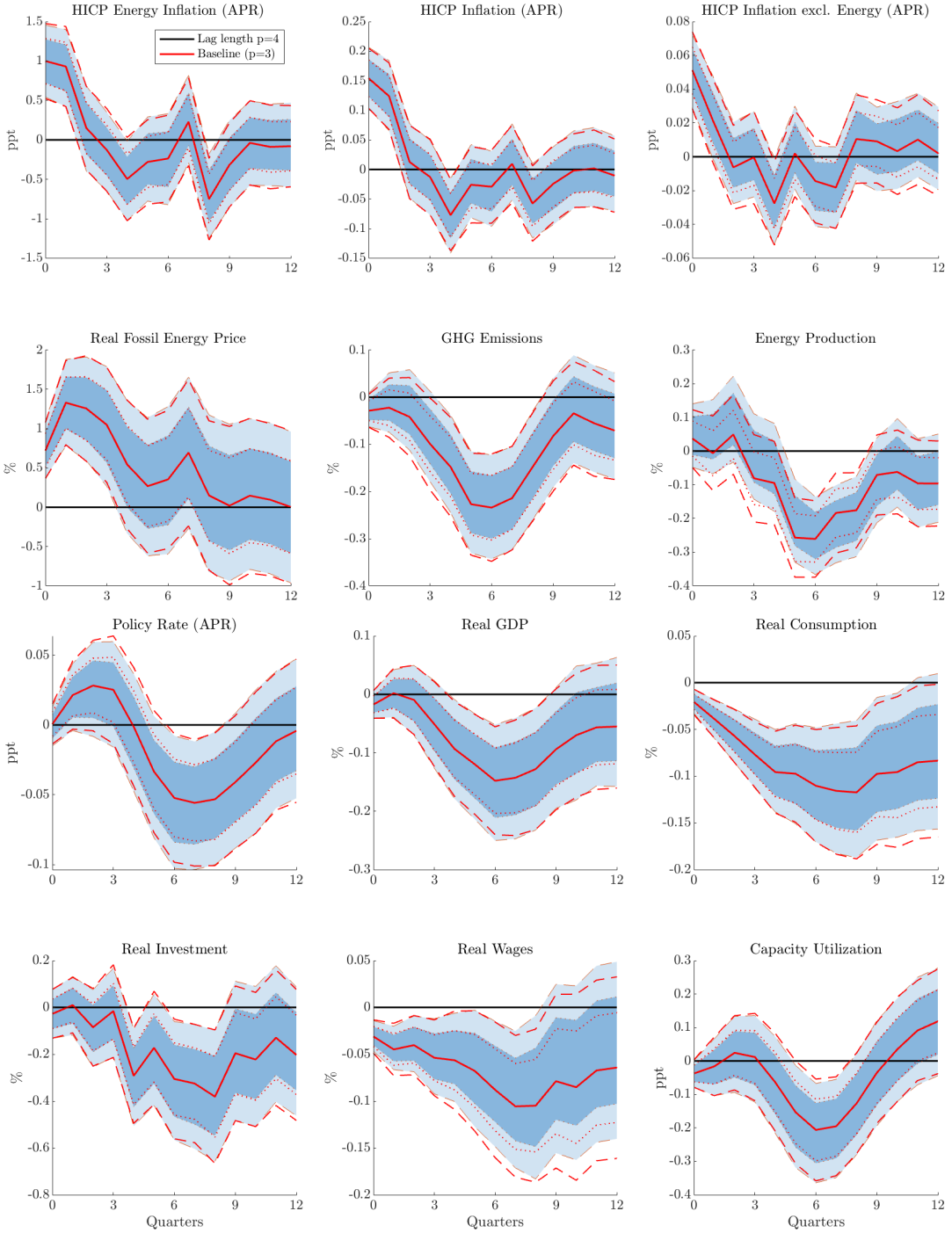


Figure B.2: Impulse responses - Alternative lag length

Notes: The solid line is the point estimate, the dark and light shaded areas are 68 and 90 % confidence bands. The baseline point estimate is depicted by the red line. The dotted and dashed red lines are the baseline 68 and 90 % confidence bands. The shock is normalized to increase annual energy inflation by 1 ppt on impact.

Figure B.3 shows the impulse responses based on log-differences for the variables that are specified in log-levels in the baseline estimation. The local projections are estimated in log-differences and then cumulated to make the responses comparable to the baseline specification.

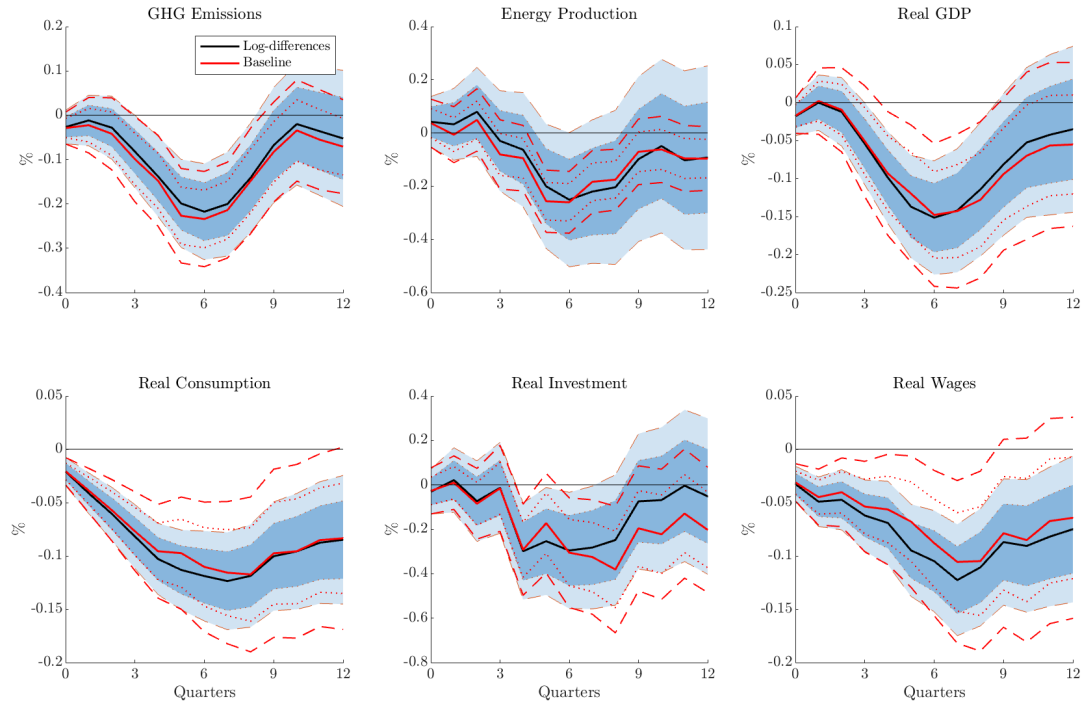


Figure B.3: Impulse responses - Estimation based on log-differnces

Notes: The solid line is the point estimate, the dark and light shaded areas are 68% and 90% confidence bands. The baseline point estimate is depicted by the red line. The dotted and dashed red lines are the baseline 68% and 90% confidence bands. The shock is normalized to increase annual energy inflation by 1 ppt on impact.

B.3 Local projections: Additional variables

Figure B.4 shows the impulse responses of real potential output and the output gap to a carbon price shock. The shock is normalized to have the same impact effect of annualized energy inflation as in the baseline estimation.

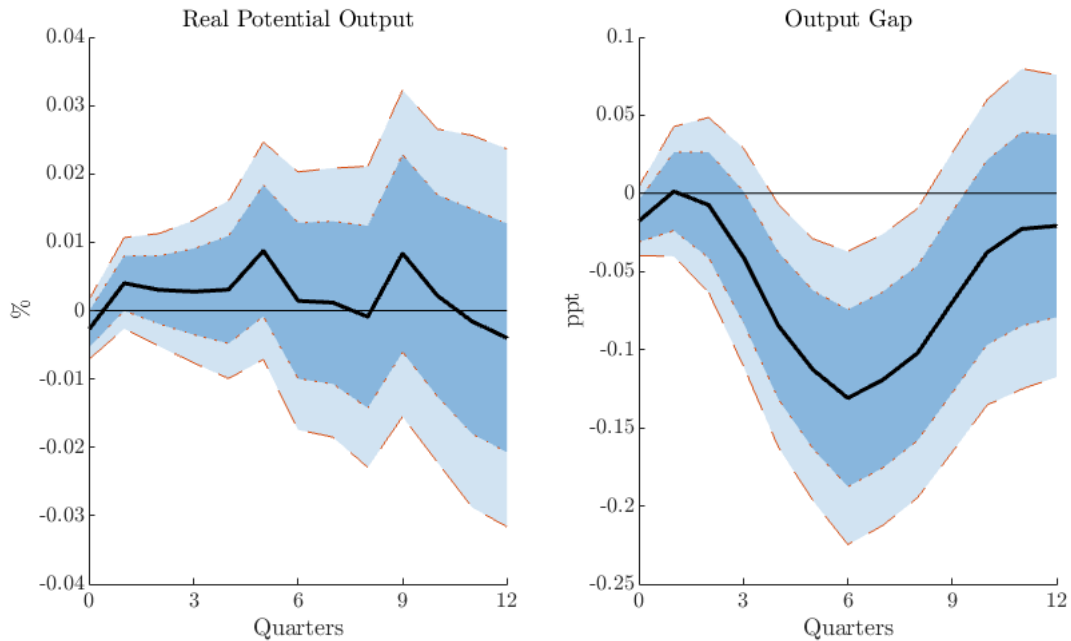


Figure B.4: Impulse responses of potential output and the output gap

Notes: The solid line is the point estimate, the dark and light shaded areas are 68% and 90% confidence bands. The shock is normalized to increase annual energy inflation by 1 ppt on impact.

C Model: Details

C.1 Optimal wage setting

I assume that each period Ricardian household i can adjust its nominal wage with constant probability $1 - \theta_w$. A household that cannot re-optimize in a given period sets its wage equal to the previous period, adjusted for steady-state inflation π , such that:

$$W_t(i) = W_{t-1}(i)\pi. \quad (\text{C.1})$$

Labor supplied by individual households is differentiated, which yields the following expression for aggregate labor supply:

$$h_{t,R} = \left(\int_0^1 h_{t,R}(i)^{\frac{\varepsilon_W - 1}{\varepsilon_W}} di \right)^{\frac{\varepsilon_W}{\varepsilon_W - 1}}. \quad (\text{C.2})$$

Cost minimization yields the following demand schedule for the labor service of household i :

$$h_{t,R}(i) = \left(\frac{W_t(i)}{W_t} \right)^{-\varepsilon_W} h_t. \quad (\text{C.3})$$

Re-optimizing households choose the wage to maximize their expected discounted utility subject to C.3. Formally, the wage setting problem reads:

$$\max_{W_t(i)} \mathbb{E}_t \sum_{k=0}^{\infty} (\theta_W \beta)^k \left\{ \ln(c_{t+k,R}(i) - bc_{t+k-1,R}(i)) - \frac{h_{t+k,R}(i)^{1+\varphi}}{1+\varphi} \right\}, \quad (\text{C.4})$$

$$\text{s.t. } h_{t+k,R}(i) = \left(\frac{W_t(i) \pi}{W_t} \right)^w h_{t+k,R} \quad \forall k \geq 0. \quad (\text{C.5})$$

Note that the demand schedule can also be rewritten as:

$$h_{t+k,R}(i) = \left(\frac{W_t(i) \pi}{P_t^R} \frac{P_{t+k}^R}{W_{t+k} P_{t+k}^R} \right)^w h_{t+k,R} \quad \forall k \geq 0. \quad (\text{C.6})$$

Solving the maximization problem yields:

$$\left(\frac{W_t(i)}{P_t^R} \right)^{1+\varepsilon_W \varphi} = \frac{\varepsilon_W}{\varepsilon_W - 1} \frac{\mathbb{E}_t \sum_{k=0}^{\infty} (\theta_w \beta)^k \left(\frac{W_{t+k}}{P_{t+k}^R} \right)^{\varepsilon_W (1+\varphi)} \left(\frac{\pi_{t+k}^R}{\pi} \right)^{\varepsilon_W (1+\varphi)} h_{t+k,R}^{1+\varphi}}{\mathbb{E}_t \sum_{k=0}^{\infty} (\theta_p \beta)^k \lambda_{t+k} \left(\frac{W_{t+k}}{P_{t+k}^R} \right)^{\varepsilon_W} \left(\frac{\pi_{t+k}^R}{\pi} \right)^{\varepsilon_W - 1} h_{t+k,R}} \quad (\text{C.7})$$

Note that in equilibrium all Ricardian households choose the same economy-wide reset

wage, i.e. $W_t(i) = W_t^*$. The above equation can thus be rewritten as:

$$\left(\frac{W_t^*}{P_t^R}\right)^{1+\varepsilon_W\varphi} = \frac{\varepsilon_W}{\varepsilon_W - 1} \frac{K_t^W}{F_t^W}, \quad (\text{C.8})$$

with K_t^W and F_t^W written recursively as:

$$K_t^W = \left(\frac{W_t}{P_t^R}\right)^{\varepsilon_W(1+\varphi)} h_{t,R}^{1+\varphi} + \beta \theta_w \left(\frac{\pi_{t+1}^R}{\pi}\right)^{\varepsilon_W(1+\varphi)} \mathbb{E}_t K_{t+1}^W, \quad (\text{C.9})$$

$$F_t^W = \left(\frac{W_t}{P_t^R}\right)^{\varepsilon_W} h_{t,R} + \beta \theta_w \left(\frac{\pi_{t+1}^R}{\pi}\right)^{\varepsilon_W-1} \mathbb{E}_t F_{t+1}^W. \quad (\text{C.10})$$

The real aggregate wage index is then given by:

$$\left(\frac{W_t}{P_t^R}\right)^{1-\varepsilon_W} = \theta_w \left(\frac{\pi_{t+1}^R}{\pi}\right)^{\varepsilon_W-1} \left(\frac{W_{t-1}}{P_{t-1}^R}\right)^{1-\varepsilon_W} + (1 - \theta_w) \left(\frac{W_t^*}{P_t^R}\right)^{1-\varepsilon_W}. \quad (\text{C.11})$$

C.2 Optimal price setting

I assume that each period firm z can adjust its price with constant probability $1 - \theta_p$. A firm that cannot re-optimize in a given period sets its price equal to the previous period, adjusted for steady-state inflation π , such that:

$$P_t^X(z) = P_{t-1}^X(z)\pi. \quad (\text{C.12})$$

Re-optimizing firms choose the price to maximize their expected discounted stream of profits while that price remains effective. Formally, the price setting problem reads:

$$\max_{P_t^X(z)} \mathbb{E}_t \sum_{k=0}^{\infty} (\theta_p \beta)^k \frac{\lambda_{t+k}}{\lambda_t} \left[\frac{P_t^X(z) \pi}{P_{t+k}^X} y_{t+k}(z) - m c_{t+k} y_{t+k}(z) \right], \quad (\text{C.13})$$

$$\text{s.t. } y_{t+k}(z) = \left(\frac{P_t^X(z) \pi}{P_{t+k}^X} \right)^{-\varepsilon} y_{t+k} \quad \forall k \geq 0. \quad (\text{C.14})$$

Here, $\beta^k \frac{\lambda_{t+k}}{\lambda_t}$ is the stochastic discount factor. Note that λ_t describes the marginal utility of Ricardian households, because they own the firms.

Solving the maximization problem yields the following first-order condition with respect to $P_t^X(z)$:

$$\mathbb{E}_t \sum_{k=0}^{\infty} (\theta_p \beta)^k \lambda_{t+k} y_{t+k} \frac{\pi}{P_{t+k}^X} \left((1 - \varepsilon) \left(\frac{P_t^X(z) \pi}{(P_{t+k}^X)} \right)^{-\varepsilon} + \varepsilon m c_{t+k} \left(\frac{P_t^X(z) \pi}{(P_{t+k}^X)} \right)^{-\varepsilon-1} \right) = 0 \quad (\text{C.15})$$

Rearranging the FOC yields:

$$P_t^X(z) = \frac{\varepsilon}{\varepsilon - 1} \frac{\mathbb{E}_t \sum_{k=0}^{\infty} (\theta_p \beta)^k \lambda_{t+k} m c_{t+k} \left(\frac{P_{t+k}^X}{\pi} \right)^\varepsilon y_{t+k}}{\mathbb{E}_t \sum_{k=0}^{\infty} (\theta_p \beta)^k \lambda_{t+k} \left(\frac{P_{t+k}^X}{\pi} \right)^{\varepsilon-1} y_{t+k}}$$

Note that in equilibrium all firms choose the same reset price, i.e. $P_t^X(z) = P_t^{X*}$. The optimal price can thus be written as:

$$P_t^{X*} = \frac{\varepsilon}{\varepsilon - 1} \frac{\bar{K}_t}{\bar{F}_t}, \quad (\text{C.16})$$

with K_t and F_t written recursively as:

$$\bar{K}_t = \lambda_t m c_t (P_t^X)^\varepsilon y_t + \beta \theta_p \pi^{-\varepsilon} \mathbb{E}_t \bar{K}_{t+1}, \quad (\text{C.17})$$

$$\bar{F}_t = \lambda_t (P_t^X)^{\varepsilon-1} y_t + \beta \theta_p \pi^{1-\varepsilon} \mathbb{E}_t \bar{F}_{t+1}. \quad (\text{C.18})$$

Now define $K_t = \frac{\bar{K}_t}{(P_t^X)^\varepsilon}$ and $F_t = \frac{\bar{F}_t}{(P_t^X)^{\varepsilon-1}}$, such that:

$$K_t = \lambda_t m c_t y_t + \beta \theta_p \mathbb{E}_t \left(\frac{\pi_{t+1}^X}{\pi} \right)^\varepsilon K_{t+1}, \quad (\text{C.19})$$

$$F_t = \lambda_t y_t + \beta \theta_p \mathbb{E}_t \left(\frac{\pi_{t+1}^X}{\pi} \right)^{\varepsilon-1} F_{t+1}. \quad (\text{C.20})$$

The resulting reset price is:

$$p_t^{X*} = \frac{P_t^{X*}}{P_t^X} = \frac{\varepsilon}{\varepsilon - 1} \frac{K_t}{F_t}. \quad (\text{C.21})$$

The real aggregate goods price index for is then given by:

$$1 = \left(\theta_P \left(\frac{\pi_t^X}{\pi} \right)^{\varepsilon-1} + (1 - \theta_P) (p_t^{X*})^{1-\varepsilon} \right)^{\frac{1}{1-\varepsilon}}. \quad (\text{C.22})$$

C.3 Equilibrium conditions

This appendix presents the full set of equilibrium conditions. All prices are expressed relative to the price of non-energy goods P_t^X . The model is described by a total of 63 equations and 63 endogenous variables $\{c_t, c_{t,R}, c_{t,H}, c_{t,R}^E, c_{t,H}^E, c_{t,R}^X, c_{t,H}^X, \lambda_t, r_t, \pi_t, \pi_t^R, \pi_t^H, \pi_t^X, \pi_t^E, r_t^{k,Y}, r_t^{k,B}, r_t^{k,G}, q_t^Y, q_t^G, q_t^B, u_t^B, u_t^Y, u_t^G, i_t, i_t^Y, i_t^G, i_t^B, k_t^Y, k_t^G, k_t^B, h_{t,R}, h_{t,H}, h_t^Y, h_t^G, h_t^B, e_t, e_t^Y, e_t^G, e_t^B, p_t, p_{t,R}, p_{t,H}, p_t^E, p_t^G, p_t^B, w_t, w_{t,R}, w_t^*, p_t^{X*}, K_t, F_t, d_t, K_t^W, F_t^W, y_t, mc_t, gdp_t, S_t, A_t^Y, A_t^G, A_t^B, \Gamma_t, \Gamma_t'\}$ and an exogenous process for τ_t .

Households:

$$\lambda_t p_t^R = \frac{1}{c_{t,R} - bc_{t-1,R}} - \beta b \mathbb{E}_t \frac{1}{c_{t+1,R} - bc_{t,R}} \quad (\text{C.23})$$

$$1 = \beta \mathbb{E}_t \frac{\lambda_{t+1}}{\lambda_t} \frac{r_t}{\pi_{t+1}^X} \quad (\text{C.24})$$

$$q_t^Y = \beta \mathbb{E}_t \frac{\lambda_{t+1}}{\lambda_t} (r_{t+1}^{k,Y} u_{t+1}^Y - a(u_t^Y) + (1 - \delta) q_{t+1}^Y) \quad (\text{C.25})$$

$$q_t^G = \beta \mathbb{E}_t \frac{\lambda_{t+1}}{\lambda_t} (r_{t+1}^{k,G} u_{t+1}^G - a(u_t^G) + (1 - \delta) q_{t+1}^G) \quad (\text{C.26})$$

$$q_t^B = \beta \mathbb{E}_t \frac{\lambda_{t+1}}{\lambda_t} (r_{t+1}^{k,B} u_{t+1}^B - a(u_t^B) + (1 - \delta) q_{t+1}^B) \quad (\text{C.27})$$

$$r_t^{k,Y} = a'(u_t^Y) \quad (\text{C.28})$$

$$r_t^{k,G} = a'(u_t^G) \quad (\text{C.29})$$

$$r_t^{k,B} = a'(u_t^B) \quad (\text{C.30})$$

$$1 = q_t^Y \left[1 - \frac{\kappa_I}{2} \left(\frac{i_t^Y}{i_{t-1}^Y} - 1 \right)^2 - \kappa_I \left(\frac{i_t^Y}{i_{t-1}^Y} - 1 \right) \frac{i_t^Y}{i_{t-1}^Y} \right] + \beta \mathbb{E}_t q_{t+1}^Y \left[\frac{\lambda_{t+1}}{\lambda_t} \kappa_I \left(\frac{i_{t+1}^Y}{i_t^Y} - 1 \right) \left(\frac{i_{t+1}^Y}{i_t^Y} \right)^2 \right] \quad (\text{C.31})$$

$$1 = q_t^G \left[1 - \frac{\kappa_I}{2} \left(\frac{i_t^G}{i_{t-1}^G} - 1 \right)^2 - \kappa_I \left(\frac{i_t^G}{i_{t-1}^G} - 1 \right) \frac{i_t^G}{i_{t-1}^G} \right] + \beta \mathbb{E}_t q_{t+1}^G \left[\frac{\lambda_{t+1}}{\lambda_t} \kappa_I \left(\frac{i_{t+1}^G}{i_t^G} - 1 \right) \left(\frac{i_{t+1}^G}{i_t^G} \right)^2 \right] \quad (\text{C.32})$$

$$1 = q_t^B \left[1 - \frac{\kappa_I}{2} \left(\frac{i_t^B}{i_{t-1}^B} - 1 \right)^2 - \kappa_I \left(\frac{i_t^B}{i_{t-1}^B} - 1 \right) \frac{i_t^B}{i_{t-1}^B} \right] + \beta \mathbb{E}_t q_{t+1}^B \left[\frac{\lambda_{t+1}}{\lambda_t} \kappa_I \left(\frac{i_{t+1}^B}{i_t^B} - 1 \right) \left(\frac{i_{t+1}^B}{i_t^B} \right)^2 \right] \quad (\text{C.33})$$

$$k_t^Y = (1 - \delta) k_{t-1}^Y + \left(1 - \frac{\kappa_I}{2} \left(\frac{i_t^Y}{i_{t-1}^Y} - 1 \right)^2 \right) i_t^Y \quad (\text{C.34})$$

$$k_t^G = (1 - \delta) k_{t-1}^G + \left(1 - \frac{\kappa_I}{2} \left(\frac{i_t^G}{i_{t-1}^G} - 1 \right)^2 \right) i_t^G \quad (\text{C.35})$$

$$k_t^B = (1 - \delta) k_{t-1}^B + \left(1 - \frac{\kappa_I}{2} \left(\frac{i_t^B}{i_{t-1}^B} - 1 \right)^2 \right) i_t^B \quad (\text{C.36})$$

$$p_t^H c_{t,H} = w_t h_{t,H} \quad (\text{C.37})$$

$$h_{t,H} = h_{t,R} \quad (\text{C.38})$$

$$p_t^R = (\gamma_{c,R}(p_t^E)^{1-\varrho_c} + (1 - \gamma_{c,R}))^{\frac{1}{1-\varrho}} \quad (\text{C.39})$$

$$p_t^H = (\gamma_{c,H}(p_t^E)^{1-\varrho_c} + (1 - \gamma_{c,H}))^{\frac{1}{1-\varrho}} \quad (\text{C.40})$$

$$c_{t,R}^E = \gamma_c \left(\frac{p_t^E}{p_t^R} \right)^{-\varrho_c} c_{t,R} \quad (\text{C.41})$$

$$c_{t,R}^X = (1 - \gamma_{c,R}) \left(\frac{1}{p_t^R} \right)^{-\varrho_c} c_{t,R} \quad (\text{C.42})$$

$$c_{t,H}^E = \gamma_{c,H} \left(\frac{p_t^E}{p_t^H} \right)^{-\varrho_c} c_{t,H} \quad (\text{C.43})$$

$$c_{t,H}^X = (1 - \gamma_{c,H}) \left(\frac{1}{p_t^H} \right)^{-\varrho_c} c_{t,H} \quad (\text{C.44})$$

Wage setting:

$$w_{t,R} = \frac{w_t}{p_{t,R}} \quad (\text{C.45})$$

$$w_{t,R} = \left(\theta_W \left(\frac{\pi_t^R}{\pi} \right)^{\varepsilon_W - 1} w_{t-1,R}^{1-\varepsilon_W} + (1 - \theta_W)(w_{t,R}^*)^{1-\varepsilon_W} \right)^{\frac{1}{1-\varepsilon_W}} \quad (\text{C.46})$$

$$(w_{t,R}^*)^{1+\phi\varepsilon_W} = \frac{\varepsilon_W}{\varepsilon_W - 1} \frac{K_t^W}{F_t^W} \quad (\text{C.47})$$

$$K_t^W = (w_{t,R}^{\varepsilon_W} h_{t,R})^{1+\phi} + \theta_W \beta \mathbb{E}_t \left(\frac{\pi_{t+1}^R}{\pi} \right)^{(1+\phi)\varepsilon_W} K_{t+1}^W \quad (\text{C.48})$$

$$F_t^W = w_{t,R}^{\varepsilon_W} h_{t,R} \lambda_t p_{t,R} + \theta_W \beta \mathbb{E}_t \left(\frac{\pi_{t+1}^R}{\pi} \right)^{(1+\phi)\varepsilon_W - 1} F_{t+1}^W \quad (\text{C.49})$$

Firms:

$$y_t d_t = \left[(1 - \gamma_Y)^{\frac{1}{\varrho_Y}} ((A_t^Y u_t^Y k_{t-1}^Y)^\alpha (h_t^Y)^{1-\alpha})^{\frac{\varrho_Y - 1}{\varrho_Y}} + (\gamma_Y)^{\frac{1}{\varrho_Y}} (e_t^Y)^{\frac{\varrho_Y - 1}{\varrho_Y}} \right]^{\frac{\varrho_Y}{\varrho_Y - 1}} \quad (\text{C.50})$$

$$w_t = m c_t ((1 - \gamma_Y) y_t d_t)^{\frac{1}{\varrho_Y}} (A_t^Y (u_t^Y k_{t-1}^Y)^\alpha (h_t^Y)^{1-\alpha})^{\frac{\varrho_Y - 1}{\varrho_Y}} (1 - \alpha) \frac{1}{h_t^Y} \quad (\text{C.51})$$

$$r_t^{k,Y} = m c_t ((1 - \gamma_Y) y_t d_t)^{\frac{1}{\varrho_Y}} (A_t^Y (u_t^Y k_{t-1}^Y)^\alpha (h_t^Y)^{1-\alpha})^{\frac{\varrho_Y - 1}{\varrho_Y}} \alpha \frac{1}{u_t^Y k_{t-1}^Y} \quad (\text{C.52})$$

$$e_t^Y = \left(\frac{p_t^E}{m c_t} \right)^{-\varrho_Y} \gamma_Y y_t d_t \quad (\text{C.53})$$

Price setting:

$$1 = \left(\theta_P \left(\frac{\pi_t^X}{\pi} \right)^{\varepsilon-1} + (1 - \theta_P) (p_t^{X*})^{1-\varepsilon} \right)^{\frac{1}{1-\varepsilon}} \quad (\text{C.54})$$

$$p_t^{X*} = \frac{\varepsilon}{\varepsilon - 1} \frac{K_t}{F_t} \quad (\text{C.55})$$

$$K_t = y_t m c_t \lambda_t + \theta_P \beta \mathbb{E}_t \left(\frac{\pi_{t+1}^X}{\pi} \right)^\varepsilon K_{t+1} \quad (\text{C.56})$$

$$F_t = y_t \lambda_t + \theta_P \beta \mathbb{E}_t \left(\frac{\pi_{t+1}^X}{\pi} \right)^{\varepsilon-1} F_{t+1} \quad (\text{C.57})$$

$$d_t = (1 - \theta_P) (p_t^{X*})^{-\varepsilon} + \theta_P \left(\frac{\pi_t^X}{\pi} \right)^\varepsilon d_{t-1} \quad (\text{C.58})$$

Energy firms:

$$e_t = \left((1 - \zeta)^{\frac{1}{\xi}} (e_t^G)^{\frac{\xi-1}{\xi}} + \zeta^{\frac{1}{\xi}} (e_t^F (1 - \Gamma_t))^{\frac{\xi-1}{\xi}} \right)^{\frac{\xi}{\xi-1}} \quad (\text{C.59})$$

$$e_t^F = \zeta \left(\frac{p_t^B (1 + \tau_t)}{p_t^E (1 - \Gamma_t - \Gamma'_t e_t^F)} \right)^{-\xi} \frac{e_t}{1 - \Gamma_t} \quad (\text{C.60})$$

$$e_t^G = (1 - \zeta) \left(\frac{p_t^G}{p_t^E} \right)^{-\xi} e_t \quad (\text{C.61})$$

$$\Gamma_t = \frac{\kappa_E}{2} \left(\frac{e_t^F}{e_{t-1}^F} - 1 \right)^2 \quad (\text{C.62})$$

$$\Gamma'_t = \kappa_E \frac{1}{e_{t-1}^F} \left(\frac{e_t^F}{e_{t-1}^F} - 1 \right) \quad (\text{C.63})$$

$$e_t^B = A_t^B (u_t^B k_{t-1}^B)^{\alpha_E} (h_t^B)^{1-\alpha_E} \quad (\text{C.64})$$

$$e_t^G = A_t^G (u_t^G k_{t-1}^G)^{\alpha_E} (h_t^G)^{1-\alpha_E} \quad (\text{C.65})$$

$$(1 - \alpha_E) p_t^B e_t^B = w_t h_t^B \quad (\text{C.66})$$

$$(1 - \alpha_E) p_t^G e_t^G = w_t h_t^G \quad (\text{C.67})$$

$$\alpha_E p_t^B e_t^B = r_t^{k,B} u_t^B k_{t-1}^B \quad (\text{C.68})$$

$$\alpha_E p_t^G e_t^G = r_t^{k,G} u_t^G k_{t-1}^G \quad (\text{C.69})$$

Climate change:

$$S_t = (1 - \delta_S) S_{t-1} + (m_t + m^{row}), \quad (\text{C.70})$$

$$A_t^Y = e^{-\psi S_t} \quad (\text{C.71})$$

$$A_t^B = e^{-\psi S_t} \quad (\text{C.72})$$

$$A_t^G = e^{-\psi S_t} \quad (\text{C.73})$$

Aggregation, market clearing and policy:

$$\frac{r_t}{r} = \left(\frac{r_{t-1}}{r} \right)^{\rho_r} \left[\left(\frac{\pi_t}{\pi} \right)^{\phi_\pi} \left(\frac{gdp_t}{gdp} \right)^{\phi_y} \right]^{(1-\rho_r)}, \quad (\text{C.74})$$

$$(1 - \lambda)h_{t,R} + \lambda h_{t,H} = h_t^Y + h_t^B + h_t^G \quad (\text{C.75})$$

$$i_t = i_t^Y + i_t^B + i_t^G \quad (\text{C.76})$$

$$e_t = e_t^Y + \lambda c_{t,H}^E + (1 - \lambda) c_{t,R}^E \quad (\text{C.77})$$

$$p_t c_t = \lambda p_{t,H} c_{t,H} + (1 - \lambda) p_{t,R} c_{t,R} \quad (\text{C.78})$$

$$p_t = \lambda p_{t,H} + (1 - \lambda) p_{t,R} \quad (\text{C.79})$$

$$y_t = c_t^X + i_t + g + \sum_j a(u_t^j) k_{t-1}^j, \quad j \in \{Y, B, G\} \quad (\text{C.80})$$

$$gdp_t = p_t c_t + i_t + g \quad (\text{C.81})$$

$$\pi_t = \frac{p_t}{p_{t-1}} \pi_t^X \quad (\text{C.82})$$

$$\pi_t^E = \frac{p_t^E}{p_{t-1}^E} \pi_t^X \quad (\text{C.83})$$

$$\pi_t^R = \frac{p_t^R}{p_{t-1}^R} \pi_t^X \quad (\text{C.84})$$

$$\pi_t^H = \frac{p_t^H}{p_{t-1}^H} \pi_t^X \quad (\text{C.85})$$

Exogenous process:

$$\log(\tau_t) = (1 - \rho_\tau) \log(\bar{\tau}) + \rho_\tau \log(\tau_{t-1}) + \epsilon_t^\tau \quad (\text{C.86})$$

D Estimation: Additional figures

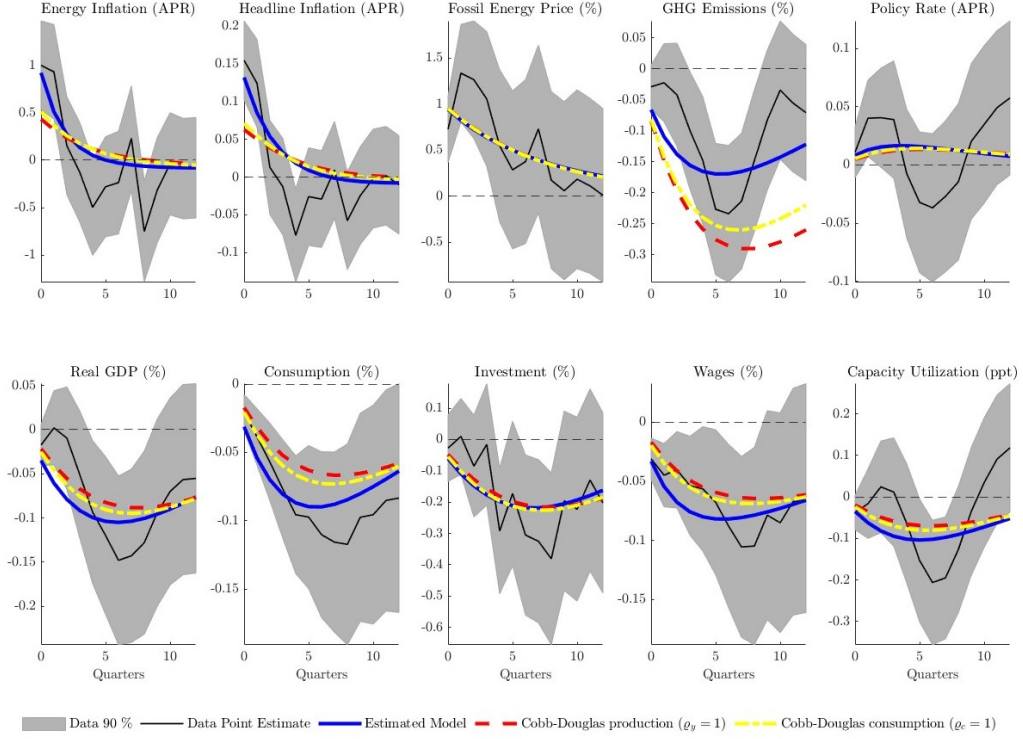


Figure D.1: Impulse responses to carbon price shock: Baseline (CES, $\varrho_y = 0.07, \varrho_c = 0.12$) vs. Cobb-Douglas production ($\varrho_y = 1$) vs. Cobb-Douglas consumption ($\varrho_c = 1$)

Notes: All other estimated parameters are kept constant to produce these impulse responses.

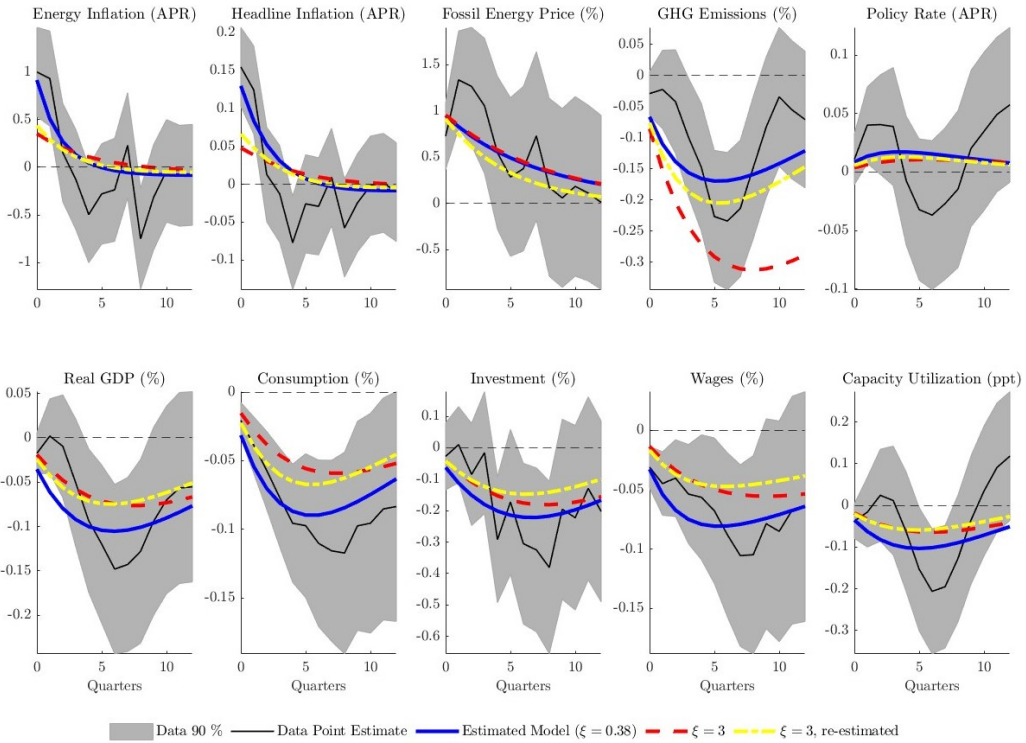


Figure D.2: Impulse responses to carbon price shock: Baseline ($\xi = 0.38$) vs. $\xi = 3$

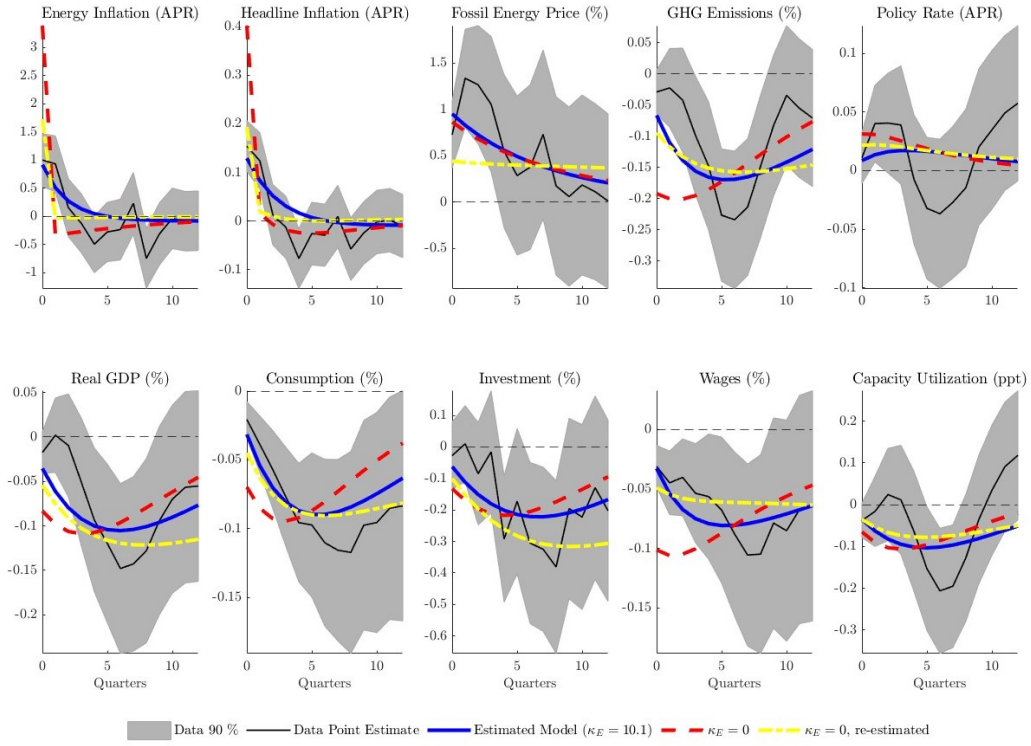


Figure D.3: Impulse responses to carbon price shock: Baseline ($\kappa_E = 10.1$) vs. $\kappa_E = 0$

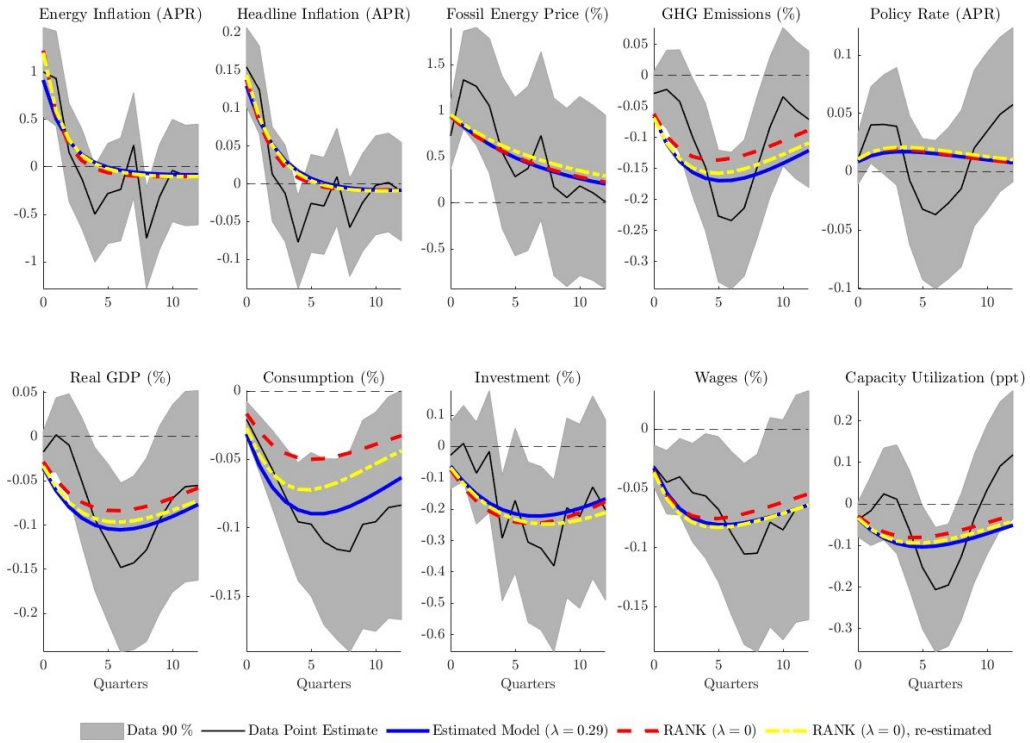


Figure D.4: Impulse responses to carbon price shock: Baseline ($\lambda = 0.25$) vs. RANK ($\lambda = 0$)

E Monetary policy: Additional figures

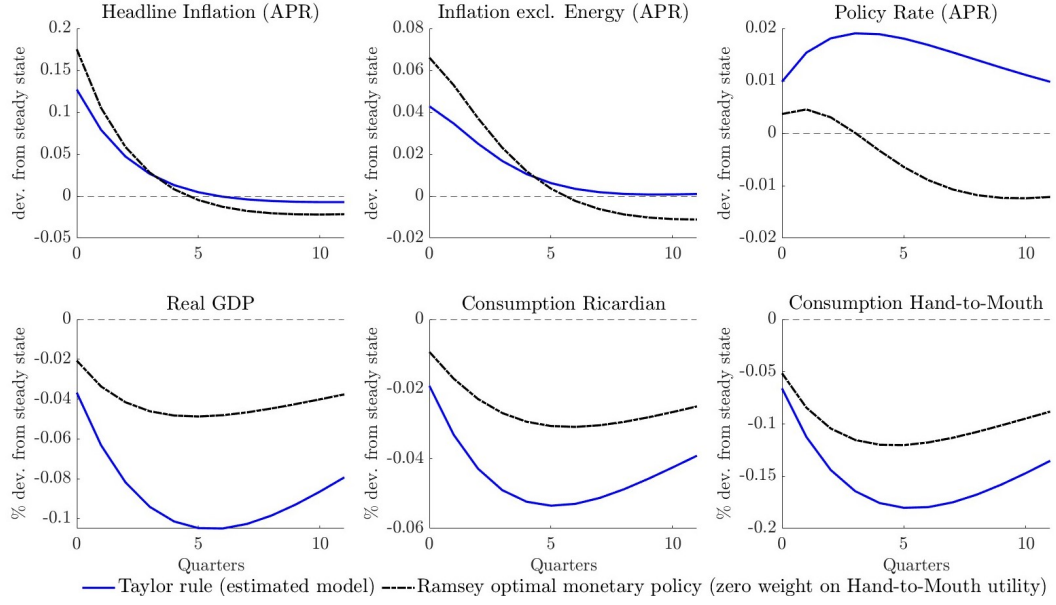


Figure E.1: Impulse responses to a carbon price shock: Estimated model with Taylor rule vs. Optimal monetary policy with zero weight on Hand-to-Mouth agents' utility

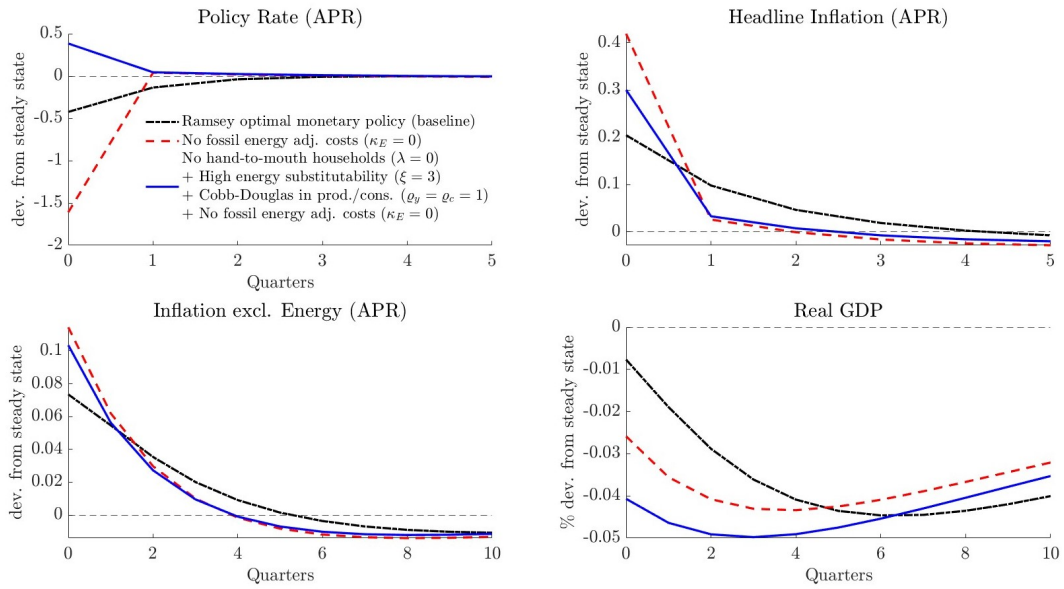


Figure E.2: Fossil energy adjustment cost as driver of the optimal monetary policy response